Journal of Medicinal Chemistry

Article

Discovery of 4,7-Diamino-5-(4-phenoxyphenyl)-6-methylene-pyrimido[5,4-b]pyrrolizines as Novel Bruton's Tyrosine Kinase (BTK) Inhibitors

Yu Xue, Peiran Song, Zilan Song, Aoli Wang, Linjiang Tong, Mei-Yu Geng, Jian Ding, Qingsong Liu, Liping Sun, Hua Xie, and Ao Zhang

J. Med. Chem., **Just Accepted Manuscript** • DOI: 10.1021/acs.jmedchem.8b00441 • Publication Date (Web): 01 May 2018

ACS Publications

is published by the American Chemical Society. 1155 Sixteenth Street N.W., Washington, DC 20036

Discovery of 4,7-Diamino-5-(4-phenoxyphenyl)-6-methylene-pyrimido[5,4-*b*]pyrrolizines as Novel Bruton's Tyrosine Kinase (BTK) Inhibitors

Yu Xue,[†,‡,∥] Peiran Song,[ǂ,Δ,∥] Zilan Song,[‡,∥] Aoli Wang,[∫] Linjiang Tong,[ǂ] Meiyu Geng,[ǂ,§,Δ] Jian Ding,[ǂ,§,Δ] Qingsong Liu,[∫] Liping Sun,[†,*] Hua Xie,[ǂ,§,*] Ao Zhang[‡,§,Δ,*]

[†]Department of Medicinal Chemistry, China Pharmaceutical University, Nanjing 210009, China

[‡]CAS Key Laboratory of Receptor Research, and the State Key Laboratory of Drug Research, Shanghai Institute of *Materia Medica*, Chinese Academy of Sciences, Shanghai 201203, China

[ǂ]Division of Anti-tumor Pharmacology, the State Key Laboratory of Drug Research, Shanghai Institute of *Materia Medica*, Chinese Academy of Sciences, Shanghai 201203, China

[∫]High Magnetic Field Laboratory, Chinese Academy of Sciences, Hefei 230031, China

[§]College of Pharmacy, University of Chinese Academy of Sciences, China

[Δ]School of Life Science and Technology, ShanghaiTech University, Shanghai 201210, China

[∥]All these authors contributed equally to this work.

*To whom correspondence should be addressed. For A.Z.: phone: +86-21-50806035; fax: 86-21-50806035; E-mail: aozhang@simm.ac.cn; For H.X.: phone: +86-21-50805897; fax: 86-21-50805897; E-mail: hxie@simm.ac.cn; For L.S.: phone: +86-25-83271414; fax: 86-25-83271414; Email: chslp@cpu.edu.cn

Abstract:

An alternative medicinal chemistry approach was conducted on BTK inhibitor **1** (ibrutinib) by merging the pyrazolo[3,4-*d*]pyrimidine component into a tricyclic skeleton. Two types of compounds were prepared, and their biochemical activities on BTK as well as stereochemistry effects were determined. Structural optimization focusing on the reactive binding group to BTK Cys481 and on the metabolic site guided by metabolic study were conducted. **7S** was identified as the most potent showing an IC_{50} value of 0.4 nM against BTK and 16 nM against BTK-dependent TMD8 cells. Compared to **1**, **7S** was slightly more selective with strong inhibition on B-cell receptor signaling pathway. In TMD8 cell-derived animal xenograft model, **7S** showed Relative Tumor Volume of 5.3 at 15 mg/kg QD dosage that was more efficacious than **1** (RTV 6.6) at higher dose of 25 mg/kg QD. All these results suggest **7S** as a new BTK inhibitor worthy of further profiling.

INTRODUCTION

The Bruton's tyrosine kinase (BTK) protein is a nonreceptor tyrosine kinase belonging to the Tec kinase family (the other members are BMX, ITK, TEC and TXK).[1] It plays a critical role in B-cell receptor (BCR) signaling by mediating B cell development and functioning. Therefore, dysregulation of BTK generally causes severe leukemias and B-cell related lymphomas.[2] BTK is the upstream activator of multiple antiapoptotic signaling molecules and networks, and is primarily expressed in hematopoietic cells, particularly in B cells, but not in T cells or normal plasma cells.[3] The essential role of BTK in BCR signaling pathway and its restricted expression pattern warrant it as a viable and attractive therapeutic target for the treatment of B-cell malignancies.[4] The first-generation multi-targeted BTK inhibitor ibrutinib[5] (**1**, PCI-32765) (Figure 1A) has been approved by FDA in 2013 to treat mantle cell lymphoma (MCL) and chronic lymphocytic leukemia (CLL), and various clinical trials are ongoing for new indications.[6,7] Compound **1** is an irreversible inhibitor by covalently binding to Cys481 of BTK with its acrylamido moiety. In addition, **1** also irreversibly binds to other kinases such as epidermal growth factor receptor (EGFR), ITK and TEC which might be attributed to the clinically observed adverse effects in ibrutinib-treated patients, including rash, diarrhea, arthralgias, atrial fibrillation, ecchymosis and major hemorrhage.[7] Though it is not for sure the off-targets also contribute to the clinical antitumor efficacy of **1**, the objective of the second-generation BTK inhibitors is to achieve better BTK on-target selectivity to minimize the side effects.[8] As shown in Figure 1, several compounds such as acalabrutinib[9] (**2**, ACP-196), tirabrutinib[10] (**3**, ONO/GS-4059) and spebrutinib[11] (**4**, CC-292) are being extensively studied in the clinic both for evaluation of their therapeutical efficacies and for their safety profiles. Very recently, compound **2**

possessing higher selectivity and inhibitory effect against BTK received the FDA's approval as a best-in-class treatment for CLL with a 100% response rate for patients positive for the 17p13.1 gene deletion - a subgroup of patients that typically results in a poor response to therapy and low expected clinical outcomes.[12] Intriguingly, compound **4**, another second-generation BTK inhibitor also irreversibly binding the Cys481 of BTK in high selectivity shows a clinical activity (in particular, durability of response) inferior to that of **1** or **2**.[7, 11] In addition to covalent inhibitors, several non-covalent BTK inhibitors have also been reported.[13-15] These non-covalent inhibitors could not form irreversible binding to BTK Cys481 because of absence of the reactive binding group. However, they could target the binding pocket of inactive BTK conformations through conformational changes, which offers reversible interaction and binding to BTK.[16] Although the precise reason is unclear for the different clinical outcomes of these compounds, more diverse inhibitors with both novel structures and selective on-target binding profile are needed.[17]

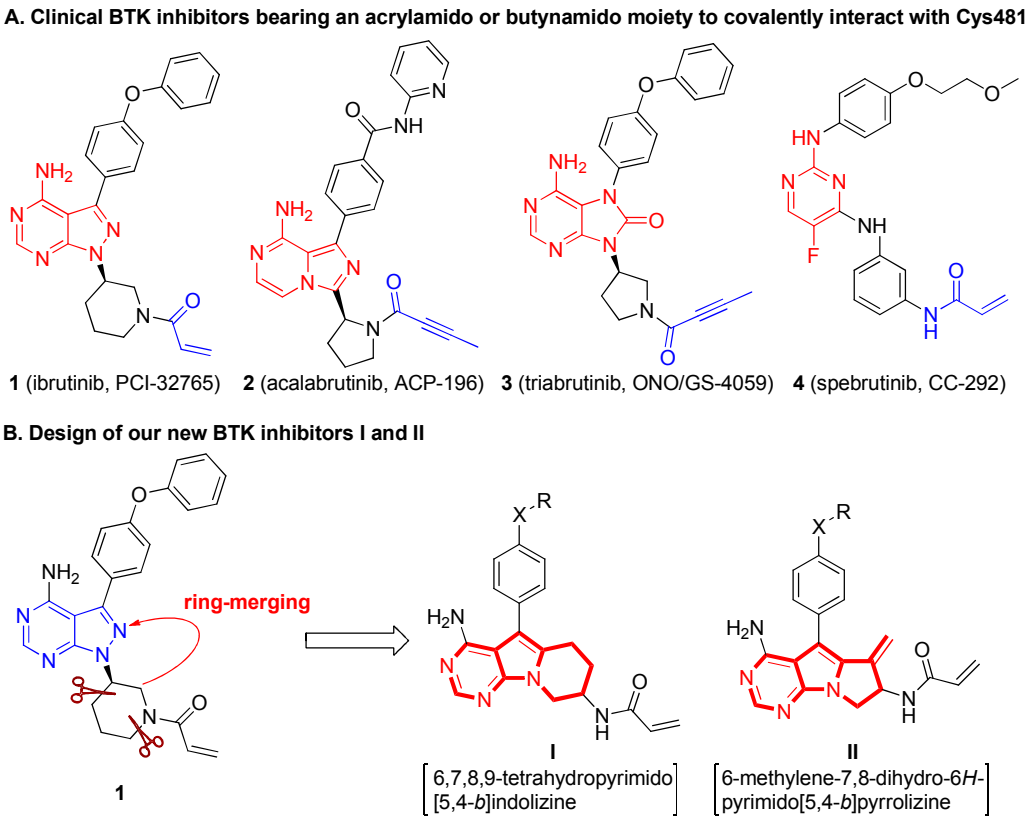

Figure 1. Clinical BTK inhibitors **1**-**4** (A) and our design of new BTK inhibitors **I** and **II** (B).

Rather than replacing the central hinge binder pyrazolo[3,4-*d*]pyrimidin-4-amine template of **1** with other bicyclic (e.g. imidazo[1,5-*a*]pyrazin-8-amine in **2** and 6-amino-7*H*-purin-8(9*H*)-one in **3**) or monocyclic (e.g. 2,4-diaminopyrimidine in **4**) bioisosteres, we recently conducted a different medicinal chemistry approach by merging the pyrazolo[3,4-*d*]pyrimidine component and the piperidine ring of **1** into a tricyclic skeleton **I** (Figure 1B). Interestingly, during the synthesis of **I**, we found that a change of the cyclization reaction condition led to a different cyclization product **II**. Both compound series **I** and **II** contain brand new core structures that are rarely seen in other categories of therapeutical drugs.[18] Herein, we report the design, synthesis, and pharmacological evaluations of both series of compounds as novel BTK inhibitors.

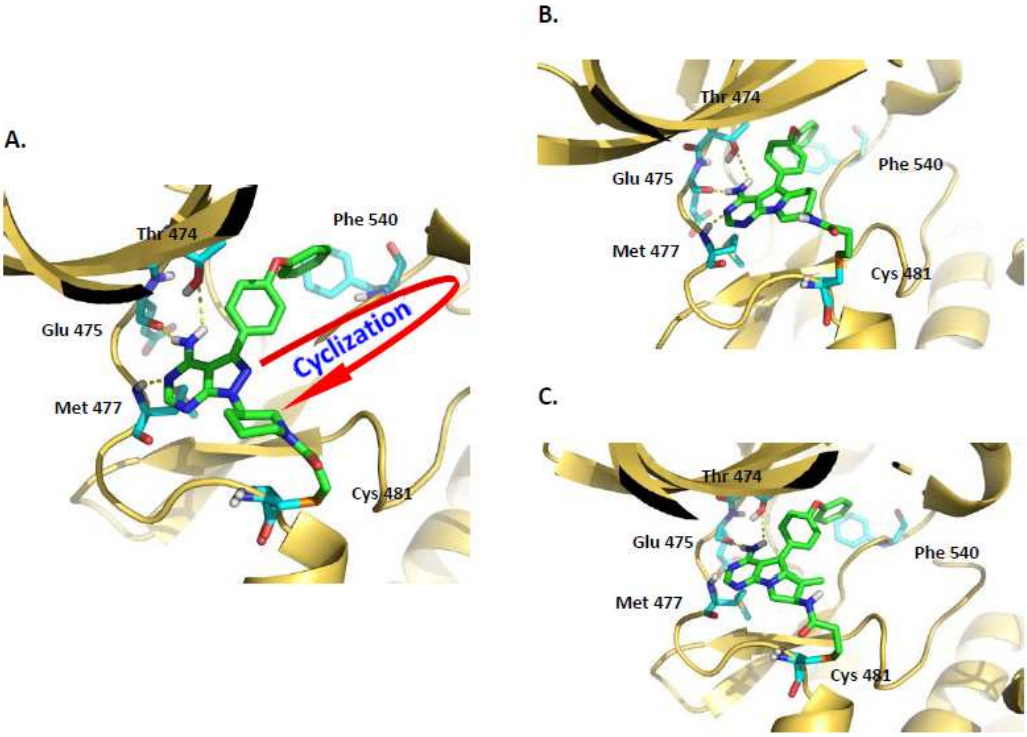

Figure 2. Binding modes of compounds **1** (A), **5** (B) and **7** (C) with BTK (PDB id: 3GEN).

RESULTS AND DISCUSSION

Structure-Based Drug Design. From the covalent docking model of **1** to BTK (PDB id: 3GEN),[19] the acrylamido moiety covalently binds to the Cys481 in the active site of BTK to achieve a potent and irreversible inhibition (Figure 2A). In addition, the pyrazolo[3,4-*d*]pyrimidine backbone of **1** forms three critical hydrogen bonds with hinge residues Met477, Glu475 and Thr474, respectively, through an edge-to-face π-π interaction between the terminal phenyl group and Phe540 in the hydrophobic pocket. The pyrazolopyrimidine backbone of **1** proves to be effective in developing BTK inhibitors, and a dozen of mimetics (e.g. **2**-**4**) of this bicyclic framework have been reported.[20] A close examination of the binding mode of **1** with BTK reveals to us that there is a large space between the nearly orthogonal pyrazolyl and piperidyl groups, indicating that occupying this space with an appropriate ring might be well tolerated. Initially, we considered to directly cyclize the pyrazolyl and

piperidyl moieties of **1** to form a tetracyclic artwork. However, consideration of the potential ring tension and the synthetic difficulty of the proposed tetracyclic backbone, a cut-off of the piperidyl ring is necessary, thus leading to our first design of the tricyclic compound series **I** (Figure 1B).

Preliminary Evaluation of Compounds 5-7. The tricyclic compound **5** was synthesized as a prototypic representative of compound series **I**. The tricycle pyrimido[5,4-*b*]pyrrolizine **7** (compound series **II**) was also obtained during optimization of the cyclization reaction condition. A docking of **5** to BTK was shown in Figure 2B, in which the critical irreversible binding, key hydrogen bonds and hydrophobic interaction as that showed in **1** were all retained. Interestingly, compound **7** bearing an exocyclic double bond also maintained the key interactions with BTK (Figure 2C) and the exocyclic double bond had no significant contacts in the catalytic domain. This analysis suggested that compounds **5** and **7** might be potent BTK inhibitors.

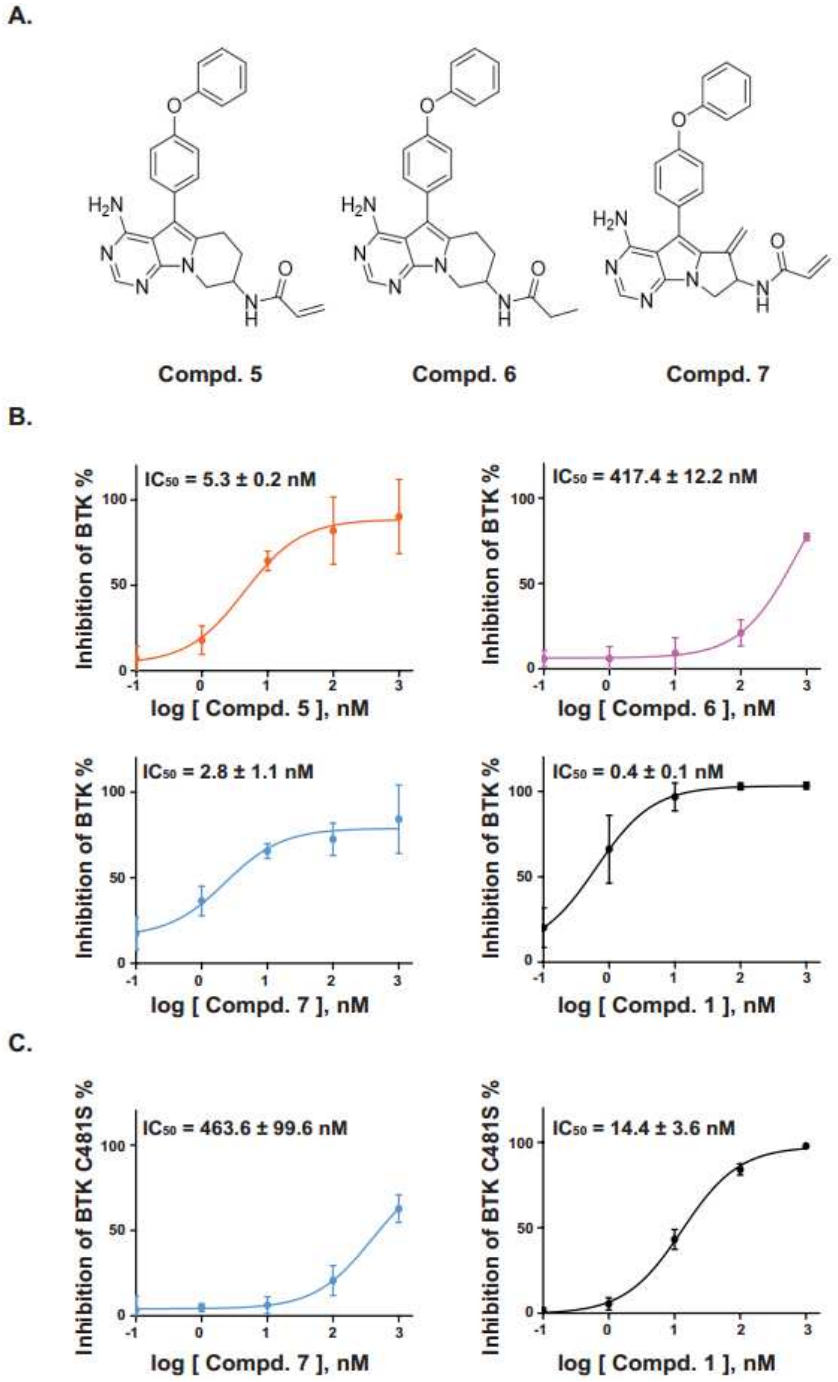

Figure 3. Characterizations of compounds **5-7** as potent BTK inhibitors. (A) Chemical structures of **5-7**. (B) *In vitro* kinase inhibitory activities of compounds against wild-type BTK. (C) *In vitro* kinase inhibitory activities of compounds **7** and **1** against BTK^{C481S} mutant.

BTK inhibitory activity of compounds **5** and **7** were evaluated by using

well-established ELISA assays. The saturated compound **6** was prepared as a comparison and compound **1** (ibrutinib) was included as a positive control (Figure 3A). As shown in Figure 3B, compounds **5** and **7** bearing an acrylamido moiety were highly potent BTK inhibitors with IC_{50} values of 5.3 nM and 2.8 nM, respectively, which were only 13-fold and 7-fold less potent than **1**. Compound **6** bearing a nonreactive propylamido moiety was approximately 1040-fold less potent (IC_{50} of 417.4 nM) than **1**. The significant discrepancy in biochemical activity between **5** and **6** illustrated the necessity of the acrylamido warhead for irreversible covalent binding with BTK Cys481. The effects of compound **7** against BTK^{C481S} mutant were further examined (Figure 3C). Compared to the high potency against wild-type BTK, compound **7** exhibited 165-fold reduction of potency against BTK^{C481S} (IC_{50} of 463.6 *vs* 2.8 nM). These results suggested that the new tricyclic compounds **5** and **7** were potent BTK inhibitors and might covalently bind to the Cys481 leading to irreversible inhibition on BTK kinase activity, a similar interaction profile to that of **1**.[5]

Kinase Selectivity Study of Compounds 5 and 7. To determine possible off-targets, we further analyzed the kinase selectivity of the two new BTK inhibitors **5** and **7** by the KINOMEScan™ screening platform.[21] Both compounds were tested against a panel of 468 kinases and mutants at 1 μM concentration and the results were showed in Figure 4. Compound **7** was found to possess a better selectivity (S-score (1) = 0.007), whereas the S(1) value of **5** was 0.027. Not surprisingly, the major off-targets of both compounds were those kinases bearing a cysteine residue in the ATP binding pocket similar to BTK, which could be covalently bound by the acrylamido warhead, including BLK, EGFR, EebB4, TEC and so on. More specifically, compound **7** had only three major off-targets (BLk, ErbB4, MEK) with a percent control number less than 1 at 1 μM concentration, a selectivity profile much

better than that of compounds **5** and **1**.[9b]

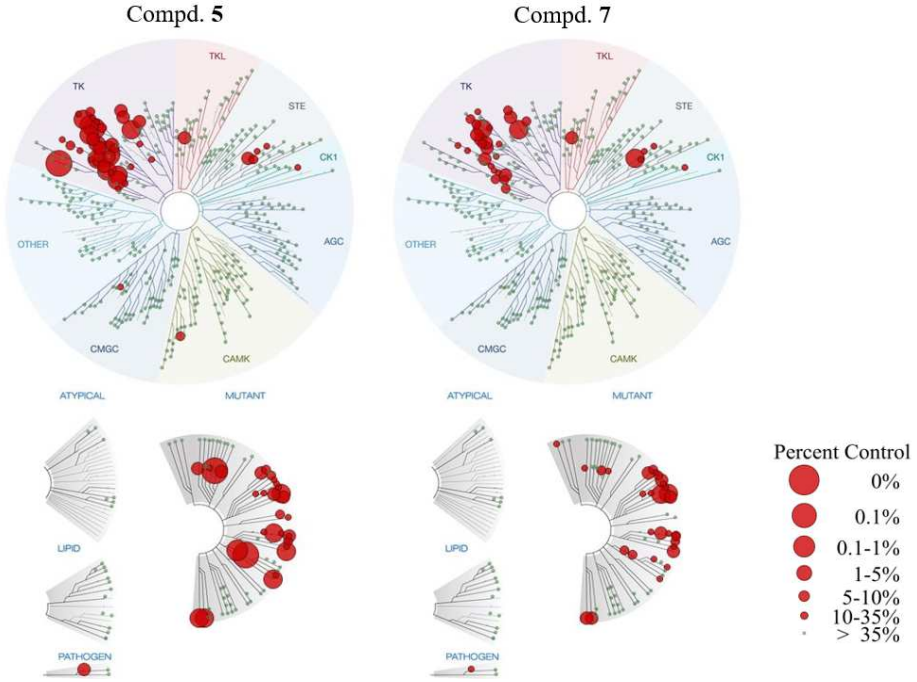

Compd.	Selectivity Score Type	Number of Hits	Number of Non-Mutant Kinases	Selectivity Score
5	S(35)	47	403	0.117
	S(10)	30	403	0.074
	S(1)	11	403	0.027
7	S(35)	33	403	0.082
	S(10)	19	403	0.047
	S(1)	3	403	0.007

Figure 4. Human kinome wide selectivity profiling of compounds **5** and **7** in DiscoveRx KINOMEScan™ screening platform. Measurements were performed at 1 μM concentration of the compounds. Upper panel: TREE*spot*™ interaction maps for **5** and **7** in 468 kinase targets. Lower panel: S-scores of **5** and **7** with percent control numbers less than 35, 10 and 1, respectively.

Structure Optimization on Lead Compound 7. In view of the structural novelty, high potency and better kinase selectivity profile, we selected compound **7** as our tricyclic lead BTK inhibitor for further structural optimization. First, to identify the

optimal covalent warhead binding to BTK Cys481 residue, a panel of reactive acrylamido groups was tested (Table 1). First, we inserted variant amino acid moieties into the acrylamido fragment and the corresponding compounds **8-11** showed reduced potencies against BTK. Compared to compound **7**, insertion of smaller amino acid moieties such as 2-aminoacetyl (**8**, IC_{50} of 23.6 nM), 2-aminopropanoyl (**9**, IC_{50} of 40.1 nM) or 1-aminocyclopropanecarbonyl (**10**, IC_{50} of 23.8 nM) led to 8- to 14-fold loss of potency, and insertion of a longer amino acid moiety such as 3-aminopropanoyl (**11**, IC_{50} of 725.2 nM) significantly reduced the inhibitory potency. Substitution on the terminal vinyl carbon with a dimethylaminomethyl yielded compound **12**, which retained high potency with an IC_{50} value of 4.3 nM. Notably, replacing the acrylamido moiety in **7** with a but-2-ynamido moiety provided compound **13** showing an IC_{50} value of 2.1 nM, a potency even higher than that of **7** (IC_{50} of 2.8 nM). Compound **14** lacking the acryloyl warhead completely lost the potency (IC_{50} > 1000 nM), whereas saturation of the acrylamido with nonreactive propionyl moiety led to 22-fold reduction of potency (**15**, IC_{50} of 62.6 nM). These results further confirmed that the existence of a Michael acceptor warhead was essential for BTK's covalent binding, and the but-2-ynamido (**13**, IC_{50} of 2.1 nM) was slightly better than the prototypic acrylamido moiety (**7**, IC_{50} of 2.8 nM).

Table 1. The *in vitro* BTK inhibition of compounds bearing different covalent or noncovalent reactive groups.

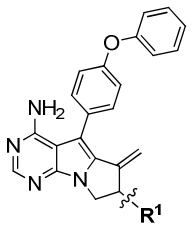

Compd.	R^1	BTK IC_{50} (nM)[a]

7	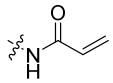	2.8 ± 1.1
8	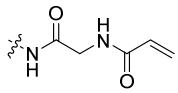	23.6 ± 4.5
9	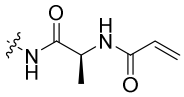	40.1 ± 4.7
10	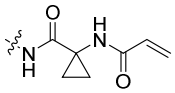	23.8 ± 5.0
11	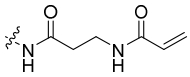	725.2 ± 182.5
12	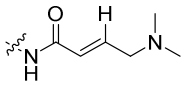	4.3 ± 0.7
13	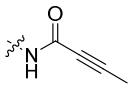	2.1 ± 0.2
14		> 1000
15	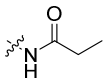	62.6 ± 13.4

[a]IC_{50} values are reported as means of duplicates.

Chiral Resolution of Potent BTK inhibitors 5, 7 and 13. Since compound **1** is an optically pure *R*-enantiomer in the stereogenic carbon center, its *S*-enantiomer as well as the racemate are less potent.[5a] To determine where this was also the case in our new tricyclic BTK inhibitors, the *R*- and *S*-enantiomers of the three potent racemic compounds **5**, **7** and **13** were prepared and tested. As shown in Table 2, enantiomers **5R** and **5S** showed nearly identical IC_{50} values (3.0 *vs* 2.8 nM). Surprisingly, significant discrepancy was observed between the two enantiomers of **7** and **13** both bearing the pyrimido[5,4-*b*]pyrrolizine framework. In both cases, the

S-enantiomers were more potent than their corresponding *R*-enantiomers. Both **7S** and **13S** showed high potency with an identical IC_{50} value of 0.4 nM, which was equal to that of **1** (IC_{50} of 0.4 nM), whereas the IC_{50} values of *R*-enantiomers **7R** and **13R** were 6.1 and 3.3 nM, respectively. The similar biochemical activity of the enantiomers **5S** and **5R** on BTK binding is likely ascribed to the fact that the newly formed piperidine ring in **5** could torture to adapt a configuration change upon covalently binding to the active site of BTK. However, the newly formed pyrrole ring in **7** and **13** have more ring and steric strain that is disadvantageous for ring tortuosity.

Table 2. The *in vitro* BTK inhibition of the stereoisomers of potent compounds **5**, **7** and **13**.

Compd.	Configuration	BTK IC_{50} (nM)[a]
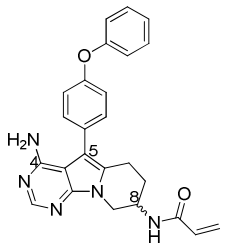	**5** (racemate)	5.3 ± 0.2
	5R (*R*-enantiomer)	3.0 ± 1.9
	5S (*S*-enantiomer)	2.8 ± 0.3
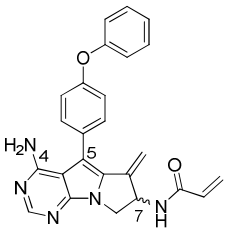	**7** (racemate)	2.8 ± 1.1
	7R (*R*-enantiomer)	6.1 ± 1.4
	7S (*S*-enantiomer)	0.4 ± 0.1
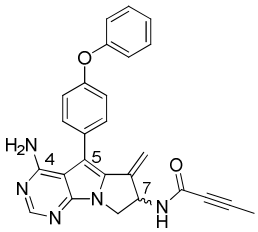	**13** (racemate)	2.1 ± 0.2
	13R (*R*-enantiomer)	3.3 ± 1.1
	13S (*S*-enantiomer)	0.4 ± 0.1

[a]IC_{50} values are reported as means of duplicates.

Pharmacokinetic (PK) Parameters of the Selected BTK Inhibitors 7S and 13S. Since both **7S** and **13S** showed high potencies against BTK kinase, they were selected for pharmacokinetic study in rats following intravenous (1 mg/kg) and oral (3 mg/kg) administration. As a comparison, **1** was also tested in the same conditions. As shown in Table 3, both **7S** and **13S** have similar half-lives ($T_{1/2}$ = 0.57 h and 0.54 h, respectively), which were slightly longer than that of **1** ($T_{1/2}$ = 0.42 h). Meanwhile, better plasma exposure after oral administration was observed for both tricyclic compounds, and the $AUC_{0-\infty}$ values for **7S** and **13S** were 4- and 10-fold higher than that of **1**, respectively. The same trend was observed in their C_{max} values. In addition, both **7S** and **13S** showed lower clearances than **1**. Finally, the oral bioavailabilities of **7S** and **13S** were calculated as 18.3% and 35.8%, respectively, which were much higher than that of **1** (F = 4.00%).

Table 3. PK parameters of the new BTK inhibitors **7S** and **13S** in rats.[a]

Compd.	iv (1 mg/kg)			po (3 mg/kg)			
	CL (L/h/Kg)	V_{ss} (L/kg)	$T_{1/2}$ (h)	C_{max} (ng/mL)	T_{max} (h)	$AUC_{0-\infty}$ (ng·h/mL)	F (%)
1	61.2	1838	0.42	39	0.25	57	4.00
7S	46.3	1299	0.57	223	0.25	211	18.3
13S	32.8	1390	0.54	340	0.25	557	35.8

[a]Values are the average of three determinations. Vehicle: DMSO, Tween 80, normal saline. CL, clearance; V_{ss}, volume of distribution; $T_{1/2}$, half-life; C_{max}, maximum concentration; T_{max}, time of maximum concentration; $AUC_{0-\infty}$, area under the plasma concentration time curve; F, oral bioavailability.

Metabolic Stability Study of the Selected BTK Inhibitors 7S and 13S. To evaluate the metabolic stability of the new tricyclic BTK inhibitors **7S** and **13S**, we

investigated the potential metabolites of both compounds by incubating with liver microsomes of different species (mouse, rat and human) for three hours. The major metabolites were tested by LC/MS (supporting information, Table S1). Both compounds showed moderate to good stability with similar metabolic products in the liver microsomes. Compound **7S** was more stable in mouse liver microsomes (MLM) than in human liver microsomes (HLM) and rat liver microsomes (RLM). Differently, compound **13S** was much more stable in HLM and MLM, but not stable in RLM. In general, the major metabolic pathway for both compounds was the *para*-oxidation of the phenyl group in the diphenyl ether component leading to *para*-hydroxylated compound **M-1**, accounting for 16.5% and 18.8%, respectively, of the total metabolites (including parent compound **M-0**) in HLM (Table S1). In addition, substantial dihydroxylation occurred in both the vinyl (**7S**) and ethynyl (**13S**) moieties across the three liver microsomes. The proposed metabolic pathways of both compounds were shown in Figures 5A and 5B.

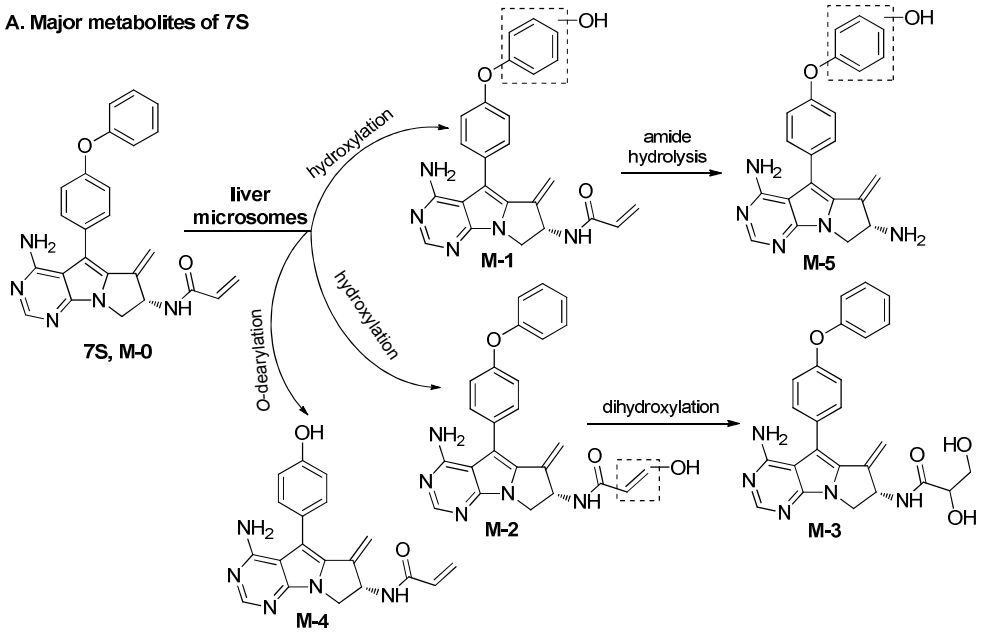

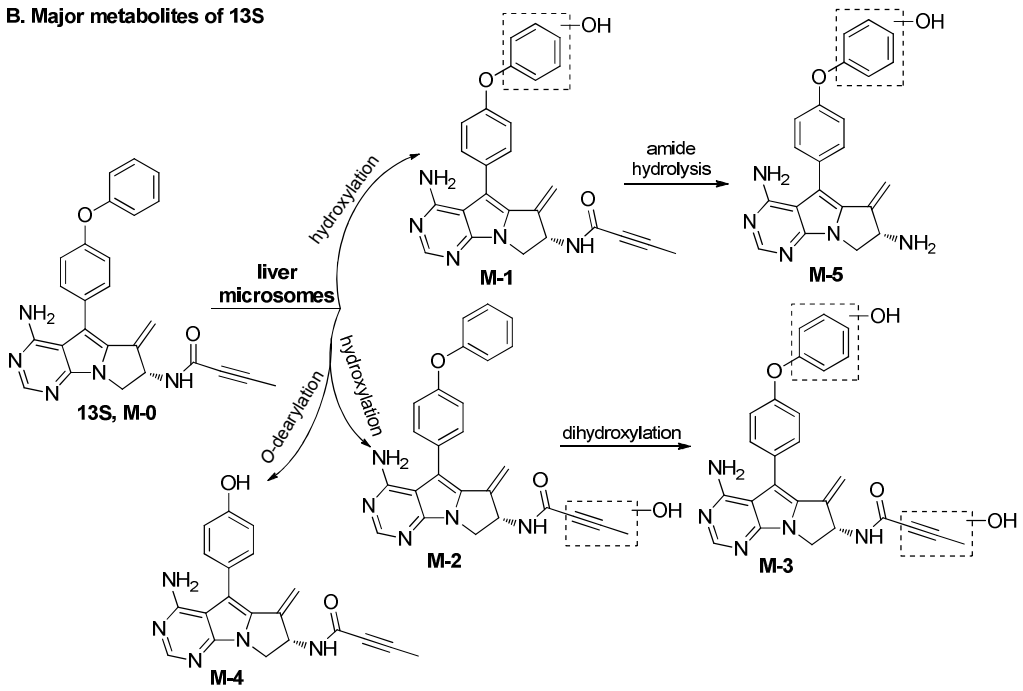

Figure 5. Metabolic study of compounds **7S** and **13S** in liver microsomes of different species.

Further Modification of Compound 7S. Since the metabolic stability study in liver microsome revealed that the most active metabolic site of compound **7S** might be the *para*-position of the terminal phenyl group. Therefore, two approaches were conducted to eliminate or ultimately reduce the *para*-phenyl oxidative metabolism (Table 4). First, we introduced a small series of substituents to the *para*-position of the terminal phenyl to block the hydroxylation liability. It was found that all the substituents, including -*t*-Bu (**16**), -F (**17**), -CF_3 (**18**) and -OCF_3 (**19**) groups, appended in the *para*-position caused 5- to 19-fold decrease of potency, comparing to that of **7S**. The reduced potency was likely due to the steric hindrance in the hydrophobic binding pocket. In the meantime, replacement of the terminal phenoxy fragment with various *N*-aryl or *N*-arylmethyl carbamic groups was conducted to block the active metabolic site. To our delight, compared to **7S**, compound **20** bearing a pyridie-2-ylcarbamic group showed compatible biochemical potency against BTK with an IC_{50} value of 0.5 nM. Compound **21** bearing an additional trifluoromethyl

group also retained high potency of 0.8 nM. Replacing the terminal phenoxy group of **7S** with (1-(pyridin-2-yl)ethyl)carbamic moiety significantly reduced the potency (**22**, IC_{50} of 50.4 nM), whereas slightly lower potency was observed for compounds **23** and **24**, both bearing a benzylcarbamic moiety and showing IC_{50} values of 3.1 nM and 4.3 nM, respectively.

Table 4. The *in vitro* BTK inhibition of compounds modified in terminal phenyl to block the *para*-oxidative metabolism.

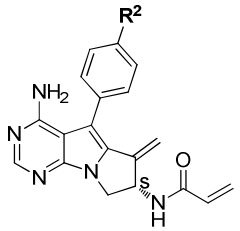

Compd.	R^2	BTK IC_{50} (nM) [a]
7S		0.4 ± 0.1
16	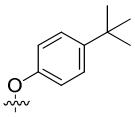	3.7 ± 0.9
17	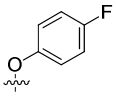	2.2 ± 1.5
18	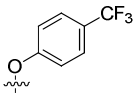	7.4 ± 2.5
19	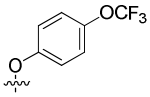	3.5 ± 1.7
20	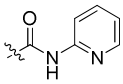	0.5 ± 0.1
21	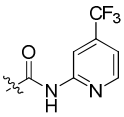	0.8 ± 0.1

22	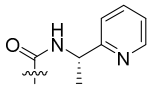	50.4 ± 9.4
23	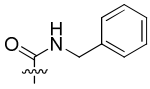	3.1 ± 1.0
24	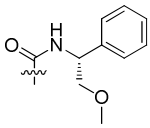	4.3 ± 1.7

[a]IC_{50} values are reported as means of duplicates.

Antiproliferative Effects of Compounds 7S, 20 and 1. Since the optimized compound **20** showed similar high potency against BTK as that of the lead compound **7S** and the approved drug **1**, both **7S** and **20** were selected for antiproliferative effect study in the B-cell lymphoma (Ramos and TMD8) cells. Compound **1** was also tested as a comparison. Both Ramos and TMD8 cells are B-cell lymphoma cell lines expressing BTK protein, but the Ramos cells are not strongly depended on it, whereas the survival of TMD8 cells is strongly dependent on the expression of BTK protein.[4b] As shown in Table 5, compounds **7S** and **20** suppressed the proliferation of Ramos cells in micromolar range with IC_{50} values of 5.03 μM and 14.3 μM, respectively, whereas the approved drug **1** showed an IC_{50} value of 0.92 μM. This result confirmed that **1** was a non-selective BTK inhibitor and its antitumor activity was a consequence of multiple kinase inhibition. The lower potency of the new inhibitors **7S** and **20** indicated that these new tricyclic compounds were more BTK-selective. This analysis was further confirmed by the high antiproliferative potency against the BTK highly sensitive TMD8 cells. All the three compounds **1**, **7S** and **20** showed low nanomolar potency with IC_{50} values of 10 nM, 16 nM and 4 nM, respectively in this cell line.

Table 5. Target inhibition and antiproliferative effects of selected compounds.

Compd.	**IC_{50} (μM)[a]**

	BTK	Ramos	TMD8
1	0.0004 ± 0.0001	0.92 ± 0.1	0.010 ± 0.004
7S	0.0004 ± 0.0001	5.03 ± 0.85	0.016 ± 0.010
20	0.0005 ± 0.0001	14.3 ± 6.1	0.004 ± 0.003

[a]IC_{50} values are reported as means of duplicates.

From the results above, both the new inhibitors **7S** and **20** showed high potency and selectivity against BTK, especially for compound **20**. Unfortunately, further pharmacokinetic study on **20** showed a lower oral bioavailability of 8.24% (Supporting Information, Table S2). Taking together, compound **7S** showed overall optimal drug candidacy and was elected for further profiling.

Covalent docking mode of 7S with BTK. Similar to binding mode of compound **7** with BTK in Figure 2C, the specific *S*-enantiomer **7S** could covalently bind to BTK Cys481. As shown in Figure 6, **7S** overlapped well with **1**, including the bicyclic skeleton as well as the hydrophobic moiety. The sulfhydryl of Cys481 rotated about 68° to adapt the newly formed covalent bond between the acrylamido moiety of **7S** and BTK Cys481. Critical hydrogen bonds with hinge residues Met477, Glu475 and Thr474 were also observed with distances of 2.0, 1.9 and 2.8 Å, respectively. In addition, there is a π-π interaction between the terminal phenyl group and Phe540.

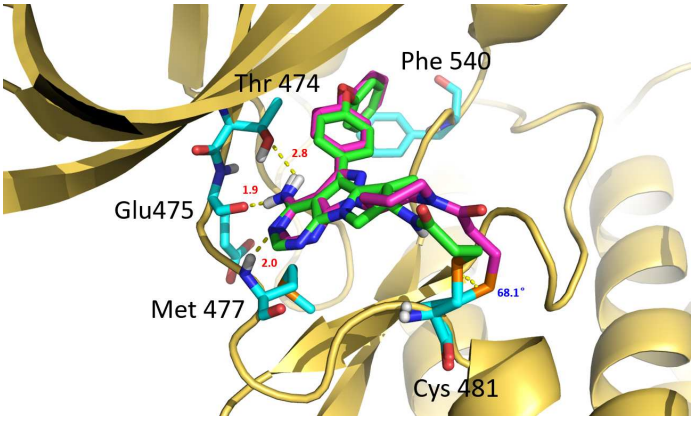

Figure 6. Covalent docking mode of compound **7S** (green) with BTK (PDB id: 3GEN)

overlapping with **1** (purple).

Kinase Selectivity Profile of 7S. On the basis of the KINOMEScan™ screening results of the racemic compound **7** (Figure 4), we further tested the biochemical activity of compound **7S** against a panel of 14 kinases. Similar to **1**, the major off-target kinases of **7S** were those with cysteine residue in the ATP binding pocket, which could be irreversibly bound by the covalent reactive group (Table 6). As such, compound **7S** showed a high potency against EGFR (IC_{50} of 1.3 nM), but variant potency against the other members of the Tec kinase family with IC_{50} values of 174.1, 15.1, 1.4 and 2.5 nM for BMX, ITK, TEC and TXK, respectively. Although the overall selectivity was similar to **1**, **7S** showed greater BTK-selectivity than **1** against BMX (174.1 vs 5.8 nM), RET (20.3 vs 5.2 nM) and ErbB2 (23.2 vs 1.5 nM). It was not clear whether such difference in kinase selectivity between **7S** and **1** was beneficial to the antitumor efficacy or clinical safety, a careful balance of the clinical outcomes should be taken if compound **7S** finally proceeds to clinical trials.

Table 6. Kinase selectivity profile of compound **7S**.

Kinase	**IC_{50} (nM)**[a]	
	7S	**1**
BTK	0.4 ± 0.1	0.4 ± 0.2
BLK	0.2 ± 0.1	0.5 ± 0.2
ErbB4	0.6 ± 0.2	1.8 ± 1.0
EGFR	1.3 ± 0.3	1.2 ± 0.3
TEC	1.4 ± 0.6	0.5 ± 0.3
TXK	2.5 ± 0.5	3.0 ± 1.8
ITK	15.1 ± 3.2	13.9 ± 1.6
RET	20.3 ± 6.6	5.2 ± 2.7
ErbB2	23.2 ± 1.5	1.5 ± 0.9

Flt-3	55.0 ± 11.7	>1000
BMX	174.1 ± 93.3	5.8 ± 2.3
PDGFR-β	214.5 ± 126.0	> 1000
EPH-A2	> 1000	> 1000
CSF1R	> 1000	> 1000

[a]IC_{50} values are reported as means of duplicates.

Effects of Compound 7S on TMD8 cells. BTK plays an imperative role in BCR signaling pathway, which is relevant to several severe leukemias and lymphomas. BCR is first activated by CD79, which causes activation of upstream kinases, such as SYK (Spleen tyrosine kinase). Then BTK is recruited to cell membrane and phosphorylated in its SH2 domain. The activated BTK then phosphorylates its substrate phospholipase γ2 (PLCγ2), leading to activation of the downstream signaling pathways, such as NF-κB and STAT3.[22] In the BTK-dependent diffuse large B-cell lymphoma (DLBCL) TMD8 cells, both compound **7S** and **1** were found to significantly inhibit the autophosphorylation of BTK at the Y223 site. Particularly, **7S** showed a dose-dependent inhibition with an IC_{50} value less than 10 nM. Furthermore, **7S** inhibited downstream phosphorylation of Y759 of PLCγ2 comparable to that of **1** at 1 μM (Figure 7A).

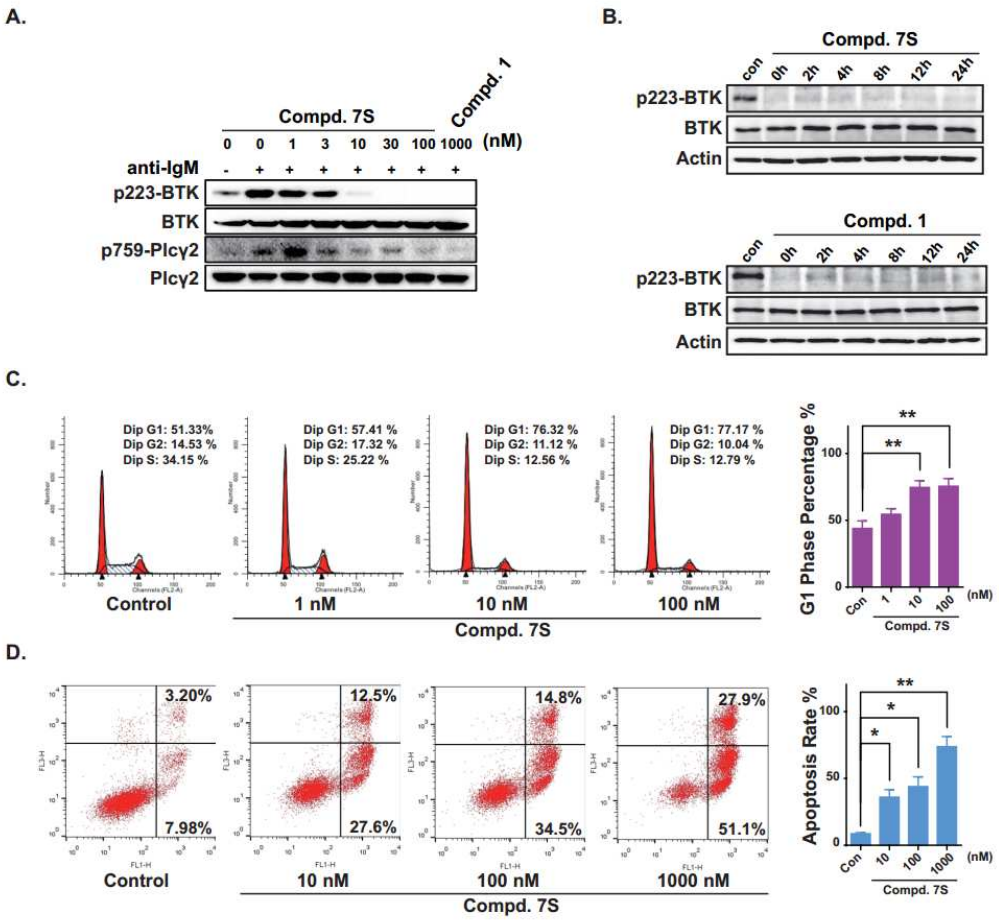

Figure 7. Effects of compound **7S** on TMD8 cells. (A) Inhibitory activity of **7S** on BTK and downstream signaling pathway in cells. Cells were starved in serum-free medium before treated with the indicated concentrations of compound **7S** or **1** for 4 h and stimulated by anti-IGM. (B) Washout experiment of **7S** in TMD8 cells. (C) Effects of **7S** on cell cycle in TMD8 cells. (D) **7S** induced apoptosis of TMD8 cells. Data are shown as mean ± SD. Each experiment was conducted independently for three times. $^{*}P < 0.05$, $^{**}P < 0.01$ *vs* control.

Meanwhile, we carried out a washout experiment to further confirm the irreversibility of compounds **7S** and **1** on the inhibition of BCR signaling pathway in TMD8 cells (Figure 7B). After 2 h exposure of **7S** and **1** at 1 μM, the cells were washed with PBS and collected in 0, 2, 4, 8, 12 and 24 h, the phosphorylated levels of BTK at Y223 were detected. The results showed that **7S** treatment for 2 h completely inhibited the phosphorylation of BTK at Y223, and the inhibition could be observed

even after 24 h washout. All these results suggested a strong irreversible inhibition of **7S** on BTK, a profile similar to that of compound **1**.

The effects of **7S** on the cell cycle progression in TMD8 cells were investigated as well. After 48 h treatment with TMD8 cells, **7S** was found to significantly arrest cell cycle progression at G1 phase in a dose-dependent manner (Figure 7C). Exposure to 1 nM of **7S** arrested 57% cells occupying the G1 phase, compared with 51% of control cells. Approximately 77% of cells was arrested in G1 phase when the concentration reached to 100 nM. We then proceeded to test the effects of **7S** on apoptosis in TMD8 cells. As illustrated in Figure 7D, **7S** triggered concentration-dependent apoptosis of the cells with ratios of 40%, 49% and 79% at concentrations of 10 nM, 100 nM and 1000 nM, respectively, compared with 11 % in untreated control cells.

Together, these results demonstrated that **7S**, as a new inhibitor of BTK, induced apoptosis and G1 phase cell cycle arrest, thus suppressing the growth of cancer cells.

Tumor Growth Inhibition of 7S in the TMD8 Xenograft Model. In view of the promising *in vitro* profile of the new BTK inhibitor **7S**, we then evaluated its antitumor activity *in vivo* in female CB-17 SCID nude mice bearing human TMD8 tumor cells. Both compounds **7S** and **1** were administered orally (po) once daily (QD) for 13 consecutive days till the vehicle group had to be euthanized due to the tumor burden. As shown in Figure 8A, oral administration of **7S** at 5 mg/kg showed minor antitumor efficacy with a Relative Tumor Volume (RTV) of 11.1. However, at a higher dose of 15 mg/kg QD, compound **7S** significantly suppressed the tumor growth with RTV of 5.3. The reference compound **1** showed a RTV of 6.6 at the dose of 25 mg/kg QD. The smaller RTV rate (5.3 vs 6.6) and lower dosage (15 vs 25 mg/kg) of **7S** over **1** indicated that compound **7S** had higher antitumor efficacy *in vivo*. Further,

the significant suppression of both **7S** and **1** on tumor growth was maintained to 17 days when the lower dosage group of **7S** (5 mg/kg) had to be euthanized. In all four groups, the mice slightly gained weight after treatment, and no significant weight fluctuations were observed during the course (Figure 8B).

We also elucidated the effects of **7S** on target inhibition in tumor by using Western blot analysis. The data shows a significant reduction of *p*-BTK expression upon D-39 treatment, accompanied with a decrease of *p*-PLCγ2 expression (Figure 8C). The expression of Ki-67, a proliferation marker in tumor,[23] was evaluated by using immunohistochemistry and H&E staining. A significant decrease of Ki-67 expression was observed in **7S** treatment group compared to the control group (Figure 8D). These results clearly demonstrated that **7S** efficiently inhibited the activation and downstream signaling transduction of BTK and thus suppressed the tumor growth.

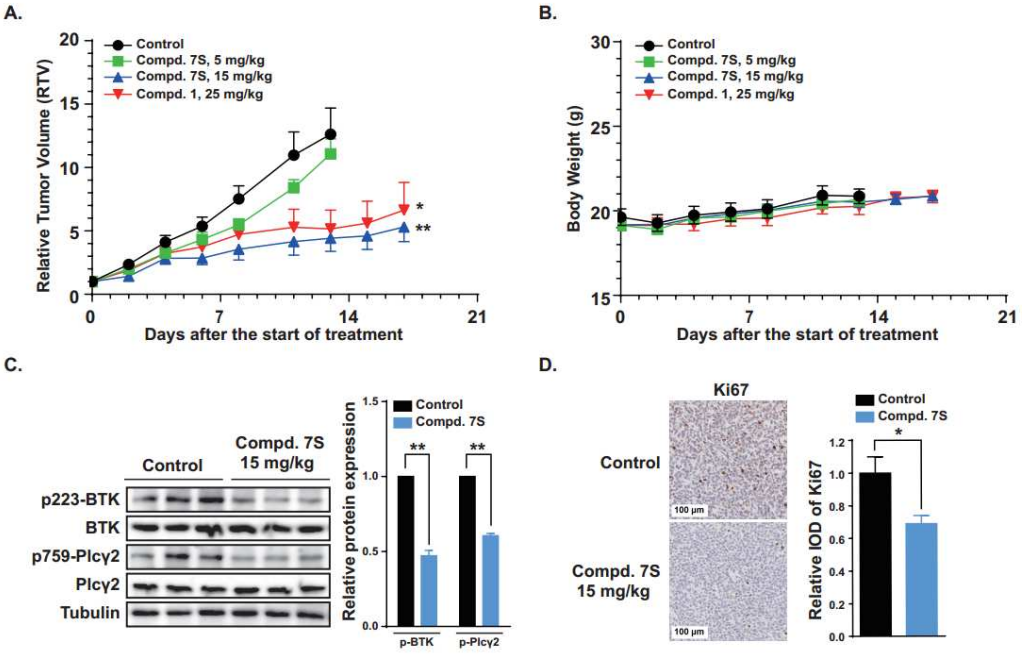

Figure 8. *In vivo* TMD8 xenograft model study of compound **7S** and **1**. (A) The tumor growth curve of four groups, including vehicle control, **1** (25 mg/kg, QD), **7S** (5 mg/kg, QD) and **7S** (15 mg/kg, QD). The vehicle group was euthanized on day 13 of treatment, and the other three groups were executed on day 17 of treatment. (B) The body weights of the group mice over time. (C)

Inhibition of target (BTK and PLCγ2) activation by **7S** in tumors. (D) Immunohistochemical analysis of Ki-67 in tumor tissues. *P < 0.05 vs. control.

CHEMISTRY

Synthesis of Tricyclic Compounds. Pyrimido[5,4-*b*]indolizine compounds **5** and **6** were prepared as shown in Scheme 1. The synthesis was started from the *O*-esterification of racemic *N*-protected alcohol **25** with methanesulfonyl chloride (MesCl) to generate the intermediate **26** in 85% yield. Substitution of 4-chloro-5-iodo-7*H*-pyrrolo[2,3-*d*]pyrimidine with aminoalcohol **26** delivered pyrrolo[2,3-*d*]pyrimidine **27** in 74% yield. Ammonolysis of **27** with ammonium hydroxide in a seal tube resulted in compound **28** in 75% yield. Pd-catalyzed Suzuki-Miyaura coupling of iodide **28** with 4-phenoxyphenylboronic acid afforded diphenyl ether **29** in 71% yield. Bromination of ether **29** with *N*-bromo succinimide (NBS) afforded bromide **30** in 84% yield. Brown hydroboration of **30** in the terminal double bond followed by intramolecular Suzuki-Miyaura coupling using $PdCl_2$dppf catalyst delivered tricyclic compound **31** in 49% overall yield. *N*-Deprotection with trifluoroacetic acid (TFA) followed by acylation with acrylic anhydride or carboxylic acid afforded compound **5** or **6** in 58% and 73% yields, respectively.

Scheme 1. Synthesis of compounds **5** and **6**.[a]

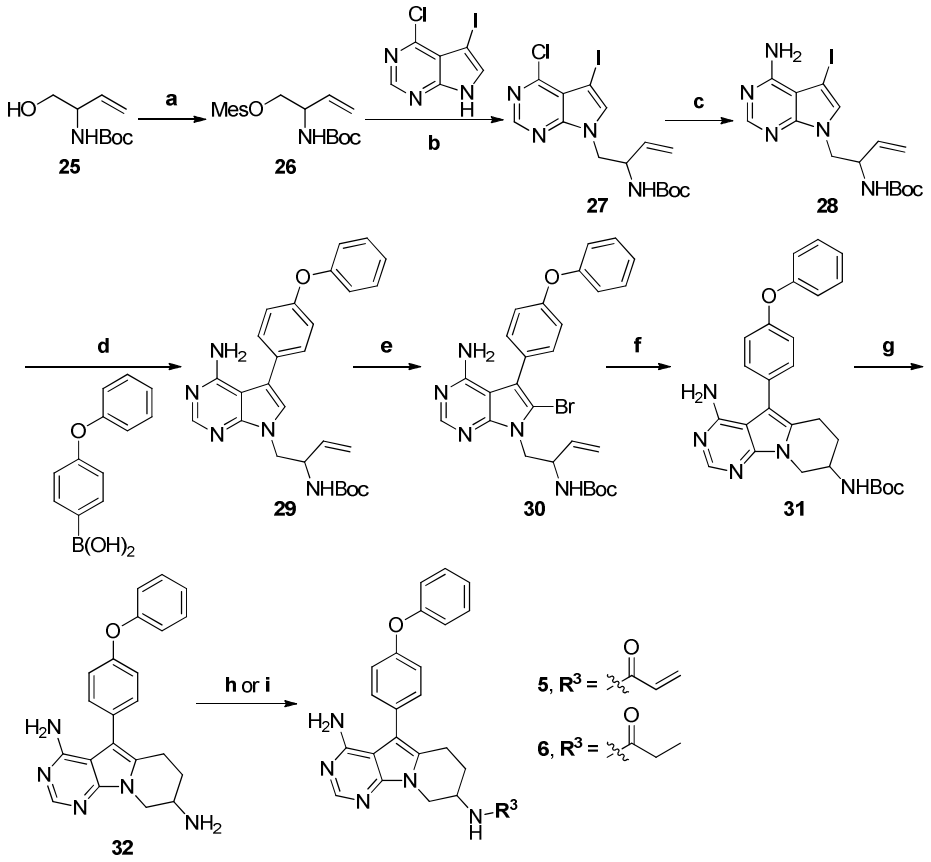

[a]Reactions and conditions: (a) MesCl, Et_3N, CH_2Cl_2, 0 °C to rt, 85%; (b) K_2CO_3, DMF, N_2, 55 °C, 74%; (c) $NH_3 \cdot H_2O$, 1,4-dioxane, 120 °C, seal tube, 75%; (d) $Pd(PPh_3)_4$, Na_2CO_3, 1,4-dioxane/H_2O, 90 °C, 71%; (e) NBS, DMF, rt, 84%; (f) 1) 9-BBN, anhydrous THF, N_2, 0 °C to rt; 2) $PdCl_2$dppf, NaOH, THF/H_2O, N_2, 85 °C, 49% (two steps); (g) TFA, CH_2Cl_2, rt; (h) acrylic anhydride, Et_3N, CH_2Cl_2, 0 °C to rt, 58% (two steps); (i) propanoic acid, HATU, Et_3N, CH_2Cl_2, rt, 73% (two steps).

It has to be mentioned that during the preparation of tricyclic compound **31**, the yield was highly dependent on the quality of boronation agent 9-borabicyclo[3.3.1]nonane (9-BBN). Lower quality of 9-BBN led to both the tricyclic **31** and **33**. After optimization of the coupling conditions, we found that compound **33** could be conveniently prepared in 88% yield through direct intramolecular Heck reaction of the precursor **30** under the catalysis of $Pd(PPh_3)_4$ (Scheme 2). After removal of the *N*-Boc protecting group of **33** with TFA, subsequent acylation with an appropriate acid or anhydride afforded the corresponding

acylamides **7-13** and **15** in 45-91% yields.

Scheme 2. Synthesis of compounds **7-15**.[a]

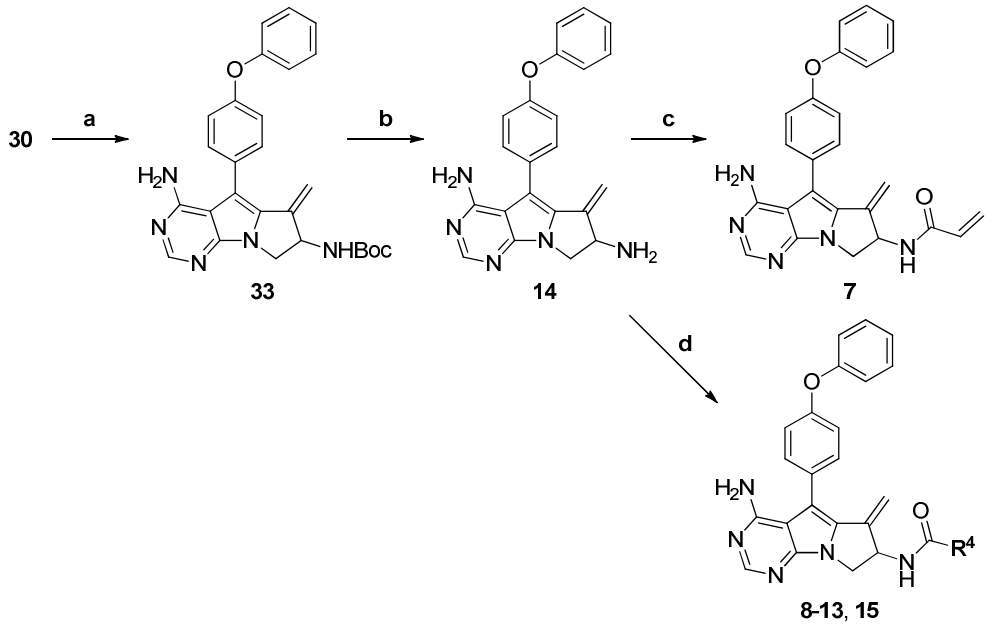

[a]Reactions and conditions: (a) $Pd(PPh_3)_4$, NaOH, THF/H_2O, N_2, 85 °C, 88%; (b) TFA, CH_2Cl_2, rt, 98%; (c) acrylic anhydride, Et_3N, CH_2Cl_2, 0 °C to rt, 45% (two steps); (d) R^4-COOH, HATU, Et_3N, CH_2Cl_2, rt, 66-91% (two steps).

Synthesis of Chiral Compounds. The optically pure isomers of compounds **5**, **7** and **13** were prepared from the *R*- or *S*-configurated isomer of **25**, which was obtained by following a literature procedure.[24] As shown in Scheme 3, phthalimide was treated with racemic 2-vinyloxirane using $Pd_2(C_3H_5)_2Cl_2$ and (*S*,*S*)-DACH-naphthyl Trost ligand leading to the *R*-configurated intermediate **34R** in a highly regio- and enantioselective fashion (yield 92%, *ee* 98%). The absolute configuration of this intermediate was confirmed by X-ray diffraction analysis (Supporting Information, Figure S1, Table S3). Subsequent treatment with CH_3NH_2 in open air in 60 °C followed by *N*-Boc protection delivered **25R**, the key intermediate for the preparation of optically pure **5R**, **7R** and **13R**. Similarly, the same reaction sequence using (*R*,*R*)-DACH-naphthyl Trost ligand afforded the *S*-configured isomer **25S**, the key

intermediate for **5S**, **7S**, **13S,** and **16-24**. Although we failed to obtain the X-ray analysis of these final compounds, a key precursor **30S** from **25S** was successfully crystallized and its X-ray analysis confirmed the absolute configuration (Supporting Information, Figure S2, Table S4).

Scheme 3. Synthesis of the *R*- or *S*-isomers of compounds **5**, **7** and **13**.[a]

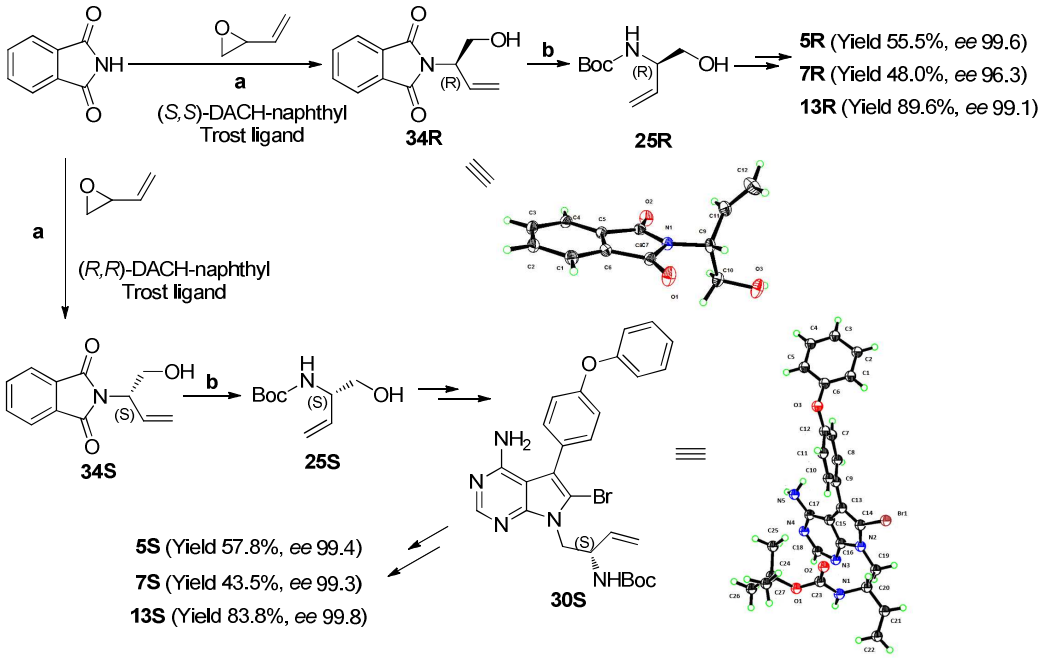

[a]Reagents and conditions: (a) $Pd_2(C_3H_5)_2Cl_2$, (*S*,*S*)-DACH-naphthyl Trost ligand for **34R** and (*R*,*R*)-DACH-naphthyl Trost ligand for **34S**, Na_2CO_3, CH_2Cl_2, N_2, rt, yield 92%, *ee* 98%; (b) 1) NH_2CH_3, open to air, 60 °C; 2) Boc_2O, $NaHCO_3$, ethyl acetate, 88% (two steps).

The synthesis of the *S*-configured compounds **16-24** was shown in Scheme 4. Suzuki-Miyaura coupling of the *S*-configured iodide **28S**, which was prepared from **25S**, with aryl boronates **35a-i** under $Pd(PPh_3)_4$ catalysis provided compounds **36a-i** in 61-85% yields. Bromination of **36a-i** followed by intermolecular Heck reaction with $Pd(PPh_3)_4$ or $PdCl_2dppf$ yielded tricyclic compounds **38a-i** in 53-81% yields. Removal of the *N*-Boc protecting group followed by acylation with acrylic anhydride provided the corresponding compounds **16-24** in 45-79% overall yields.

Scheme 4. Synthesis of chiral compounds **16-24**.[a]

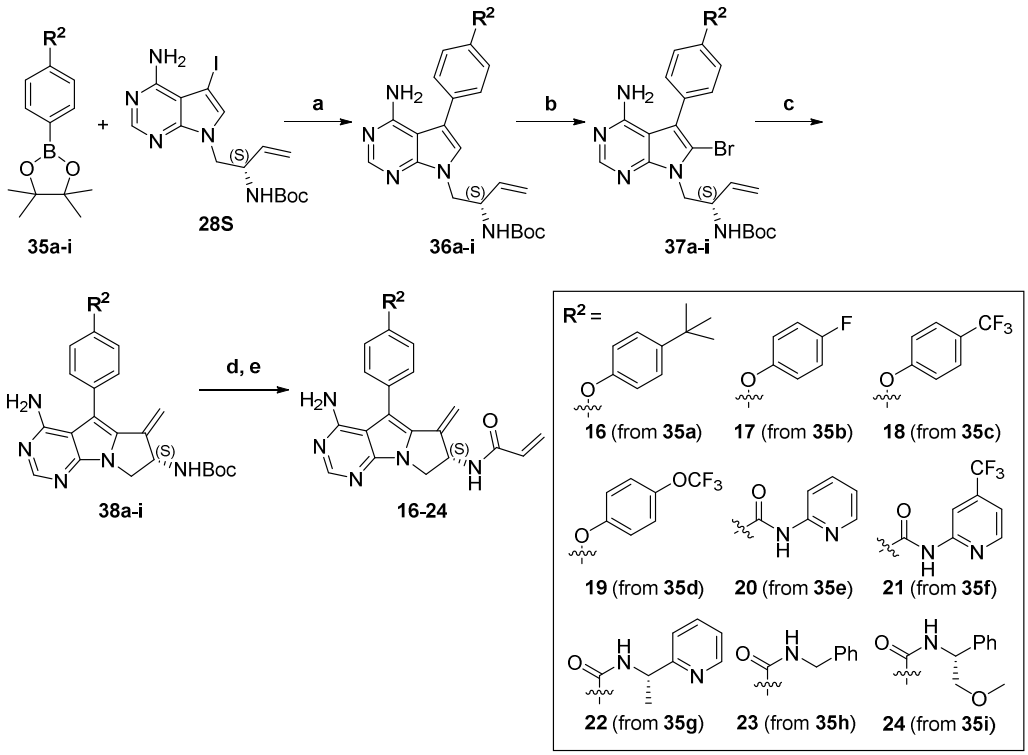

[a]Reactions and conditions: (a) $Pd(PPh_3)_4$, Na_2CO_3, 1,4-dioxane/H_2O, N_2, 90 °C, 61-85%; (b) NBS, DMF, rt, 70-77%; (c) $Pd(PPh_3)_4$ (for **16-19**) or $PdCl_2$dppf (for **20-24**), NaOH, THF/H_2O, N_2, 85 °C, 53-81%; (d) TFA, CH_2Cl_2, rt; (e) acrylic anhydride, Et_3N, CH_2Cl_2, 0 °C to rt, 45-79% (two steps).

CONCLUSIONS

In summary, using a structure-based drug design strategy, a new medicinal chemistry approach was conducted on the BTK inhibitor **1** (ibrutinib) by merging the pyrazolo[3,4-*d*]pyrimidine component and the piperidine ring **1** into a tricyclic skeleton. Two series of compounds were prepared, and their binding model, biochemical activity as well as effects of the stereochemistry on BTK were determined. Subsequent structural optimization both focusing on the reactive acrylamido group as the covalent binder to the BTK Cys481 residue and on the metabolic active site were conducted leading to the tricyclic compound **7S** as the most potent and orally available BTK inhibitor. Compound **7S** has a biochemical IC_{50} value

of 0.4 nM against BTK and antiproliferative potency of 16 nM against BTK-dependent TMD8 cells. Compared to the multi-kinase inhibitor **1**, the new inhibitor **7S** is slightly more selective against BTK, and showed strong inhibition on the BCR signaling pathway in TMD8 cells. Significant cell cycle arrest in G0-G1 phase and does-dependent inducing of apoptosis were observed as well. In the TMD8 cell-derived xenograft model, **7S** shows a Relative Tumor Volume (RTV) of 5.3 at a dose of 15 mg/kg QD that is more efficacious than compound **1** (RTV 6.6) at a higher dose of 25 mg/kg QD. In view of the novel tricyclic structure of **7S** together with its encouraging *in vitro* and *in vivo* properties, this compound is worthy of further profiling as a new BTK inhibitor. Currently, an early preclinical study on this compound has been undergoing for potential treatment of B-cell related lymphomas.

EXPERIMENTAL SECTION

Chemistry. All reactions were performed in glassware containing a Teflon coated stir bar. Commercial solvents and reagents were obtained from sources Adamas-beta, Acros Organics, Strem Chemicals, Alfa Aesar, J&K, TCI and Laajoo and used without further purification. ^{1}H and ^{13}C NMR spectra were recorded with a Varian-MERCURY Plus-300 MHz NMR spectrometer and referenced to deuterium dimethyl sulfoxide (DMSO-d_6), deuterium chloroform ($CDCl_3$) or $CDCl_3$ + deuterium methanol (CD_3OD). Chemical shifts (δ) were reported in ppm downfield from an internal TMS standard. Low- and high-resolution mass spectra were obtained in the ESI mode. Flash column chromatography on silica gel (200-300 mesh) was used for the routine purification of reaction products. The column outputs were monitored by TLC on silica gel (200-300 mesh) precoated on glass plates (15 mm × 50 mm), and spots were visualized by UV light at 254 or 365 nm. Some outputs were colored by

basic $KMnO_4$ solution. Compounds **25**, **25S**, **25R** and **35a-i** were prepared according to corresponding literature procedures.[20f, 24, 25] HPLC analysis was conducted for all biologically evaluated compounds on an Agilent Technologies 1260 series LC system (Agilent ChemStation Rev.A.10.02; ZORBAX Eclipse XDB-C18, 4.6 mm × 150 mm, MeOH/H_2O, rt; CHIRALPAK AD-H, 4.6 mm × 250 mm, *n*-hexane/*i*-PrOH or *n*-hexane/*i*-PrOH (with 0.1%(v/v) diethylamine), rt; CHIRALPAK IG, 4.6 mm × 150 mm, MeOH/diethylamine, 35 ^{o}C; CHIRALPAK IE, 4.6 mm × 250 mm, *n*-hexane/EtOAc, rt; CHIRALPAK AYH, 4.6 mm × 150 mm, *n*-hexane/EtOH/diethylamine, 35 ^{o}C) with ultraviolet wavelengths in UV 254 to determine the chemical purity and optical purity. The purities of all biologically evaluated compounds were above 95%.

Compounds **5R** and **5S** were prepared following the synthetic procedure for racemate **5** from their corresponding enantiomeric precursors.

***N*-(4-Amino-5-(4-phenoxyphenyl)-6,7,8,9-tetrahydropyrimido[5,4-*b*]indolizin-8-yl)acrylamide (5).** To a solution of compound **31** (472 mg, 1.0 mmol) in CH_2Cl_2 (20 mL) was added trifluoroacetic acid (1.9 mL) dropwise. The mixture was stirred at room temperature for 3 h, and then quenched with saturated $NaHCO_3$ solution dropwise until neutral. After extraction with CH_2Cl_2 (3 × 5 mL), the combined organic phase was washed with brine (5 mL), dried over Na_2SO_4, filtered, and concentrated in vacuo. The crude product **32** was given as yellowish solid and could be used in next step without further purification.

To a solution of compound **32** in CH_2Cl_2 (20 mL) was added acrylic anhydride (115 μL, 1.0 mmol) and Et_3N (154 μL, 1.1 mmol) at 0 ^{o}C. The mixture was stirred at 0 ^{o}C for 0.5 h. After quenching with water (5 mL) and CH_2Cl_2 (10 mL), the organic phase was separated and washed with brine (5 mL), dried over Na_2SO_4, filtered, and

concentrated in vacuo. The residue was purified by silica column chromatography ($CHCl_3$/MeOH) to give compound **5** (248 mg, 58.3%) as white solid. ^{1}H NMR (300 MHz, $CDCl_3$+CD_3OD) δ 8.07 (s, 1H), 7.32 (t, J = 8.0 Hz, 2H), 7.26 (d, J = 8.7 Hz, 2H), 7.09 (t, J = 7.4 Hz, 1H), 7.02 (d, J = 8.6 Hz, 4H), 6.31 – 6.07 (m, 2H), 5.61 (dd, J = 10.0, 1.8 Hz, 1H), 4.53 – 4.43 (m, 1H), 4.38 (dd, J = 12.3, 5.2 Hz, 1H), 3.82 (dd, J = 12.2, 8.4 Hz, 1H), 2.99 – 2.84 (m, 2H), 2.20 – 2.07 (m, 1H), 1.91 – 1.75 (m, 1H). ^{13}C NMR (126 MHz, $CDCl_3$+CD_3OD) δ 166.13, 156.86, 156.47, 156.03, 149.99, 148.89, 131.08 (2C), 130.30, 130.07, 129.86 (2C), 128.29, 126.94, 123.80, 119.35 (2C), 118.67 (2C), 110.32, 101.87, 45.28, 44.20, 26.61, 20.16. MS (ESI, $[M + H]^+$) m/z 426.3. HRMS (ESI) calcd for $C_{25}H_{24}N_5O_2$, 426.1925; found, 426.1923.

(*R*)-*N*-(4-Amino-5-(4-phenoxyphenyl)-6,7,8,9-tetrahydropyrimido[5,4-*b*]indolizin-8-yl)acrylamide (5R). White solid. Yield 236 mg, 55.5%. ^{1}H NMR (300 MHz, $CDCl_3$) δ 8.21 (s, 1H), 7.42 – 7.32 (m, 4H), 7.16 (t, J = 7.5 Hz, 1H), 7.09 (d, J = 8.3 Hz, 4H), 6.41 – 6.10 (m, 3H), 5.70 (d, J = 9.8 Hz, 1H), 4.94 (s, 2H), 4.70 (s, 1H), 4.42 (dd, J = 13.3, 5.2 Hz, 1H), 4.11 (dd, J = 13.1, 6.0 Hz, 1H), 2.98 (t, J = 6.3 Hz, 2H), 2.09 (dd, J = 15.8, 10.8 Hz, 2H). ^{13}C NMR (126 MHz, $CDCl_3$) δ 165.29, 156.84, 156.59, 155.96, 150.94, 150.01, 131.13 (2C), 130.27, 129.93 (2C), 129.29, 128.63, 127.50, 123.84, 119.44 (2C), 118.74 (2C), 110.38, 101.98, 45.95, 43.84, 26.23, 19.34. MS (ESI, $[M + H]^+$) m/z 426.3. HRMS (ESI) calcd for $C_{25}H_{24}N_5O_2$, 426.1925; found, 426.1926. $[\alpha]^{20}_D$ +87.0 (c 0.05, MeOH).

(*S*)-*N*-(4-Amino-5-(4-phenoxyphenyl)-6,7,8,9-tetrahydropyrimido[5,4-*b*]indolizin-8-yl)acrylamide (5S). White solid. Yield 246 mg, 57.8%. ^{1}H NMR (300 MHz, $CDCl_3$ + CD_3OD) δ 8.13 (s, 1H), 7.50 (d, J = 7.2 Hz, 1H), 7.39 – 7.27 (m, 4H), 7.12 (t, J = 7.3 Hz, 1H), 7.04 (d, J = 8.3 Hz, 4H), 6.36 – 6.07 (m, 2H), 5.64 (d, J = 11.5 Hz, 1H), 4.57 – 4.45 (m, 1H), 4.40 (dd, J = 12.5, 5.2 Hz, 1H), 3.85 (dd, J = 12.4, 8.4 Hz,

1H), 2.97 – 2.90 (m, 2H), 2.26 – 2.10 (m, 1H), 1.93 – 1.75 (m, 1H). ^{13}C NMR (126 MHz, $CDCl_3$ + CD_3OD) δ 165.96, 156.89, 156.51, 155.98, 150.04, 149.04, 131.10 (2C), 130.34, 130.04, 129.89 (2C), 128.31, 127.01, 123.83, 119.39 (2C), 118.71 (2C), 110.37, 101.88, 45.40, 44.17, 26.60, 20.05. MS (ESI, $[M + H]^+$) m/z 426.2. HRMS (ESI) calcd for $C_{25}H_{24}N_5O_2$, 426.1925; found, 426.1930. $[\alpha]^{20}_D$ -76.0 (*c* 0.05, MeOH).

***N*-(4-Amino-5-(4-phenoxyphenyl)-6,7,8,9-tetrahydropyrimido[5,4-*b*]indolizin-8-yl)propionamide (6).** To a solution of intermediate **32** in CH_2Cl_2 (25 mL) was added propanoic acid (81 mg, 1.1 mmol), HATU (418 mg, 1.1 mmol) and Et_3N (0.28 mL, 2.0 mmol) dropwise at 0 ^oC. The mixture was stirred at room temperature for 1.5 h and quenched with water (10 mL). After extraction with CH_2Cl_2 (3 × 5 mL), the combined organic phase was washed with brine (5 mL), dried over Na_2SO_4, filtered, and concentrated in vacuo. The residue was purified by silica column chromatography ($CHCl_3$/MeOH) to give compound **6** (312 mg, 73.0%) as white solid. ^{1}H NMR (300 MHz, $CDCl_3$) δ 8.20 (s, 1H), 7.44 – 7.30 (m, 4H), 7.16 (t, J = 7.4 Hz, 1H), 7.09 (d, J = 8.5 Hz, 4H), 5.97 (d, J = 7.5 Hz, 1H), 5.09 (s, 2H), 4.71 – 4.53 (m, 1H), 4.44 (dd, J = 12.7, 4.7 Hz, 1H), 4.00 (dd, J = 12.7, 6.7 Hz, 1H), 2.97 (t, J = 6.3 Hz, 2H), 2.26 (q, J = 15.2, 7.6 Hz, 2H), 2.14 – 1.92 (m, 2H), 1.18 (t, J = 7.6 Hz, 3H). ^{13}C NMR (126 MHz, $CDCl_3$) δ 173.66, 156.87, 156.57, 155.79, 150.45, 149.81, 131.12 (2C), 129.93 (2C), 129.51, 128.56, 123.85, 119.45 (2C), 118.75 (2C), 110.38, 101.91, 46.03, 43.65, 29.70, 26.38, 19.53, 9.87. MS (ESI, $[M + H]^+$) m/z 428.3. HRMS (ESI) calcd for $C_{25}H_{26}N_5O_2$, 428.2081; found, 428.2075.

Compounds **7R** and **7S** were prepared following the synthetic procedure for racemate **7** from their corresponding enantiomeric precursors.

***N*-(4-Amino-6-methylene-5-(4-phenoxyphenyl)-7,8-dihydro-6*H*-pyrimido[5,4-*b*]pyrrolizin-7-yl)acrylamide (7).** To a solution of intermediate **14** in CH_2Cl_2 (20

mL) was added acrylic anhydride (115 μL, 1.0 mmol) and Et_3N (154 μL, 1.1 mmol) at 0 °C. The mixture was stirred at 0 °C for 0.5 h. After completion, the mixture was added water (5 mL) and CH_2Cl_2 (10 mL). The organic phase was separated and washed with brine (5 mL), dried over Na_2SO_4, filtered, and concentrated in vacuo. The residue was purified by silica column chromatography ($CHCl_3$/MeOH) to give compound **7** (191 mg, 45.1%) as white solid. ^{1}H NMR (300 MHz, $CDCl_3$ + CD_3OD) δ 8.08 (s, 1H), 7.37 (d, J = 8.7 Hz, 2H), 7.35 – 7.29 (m, 2H), 7.14 – 7.06 (m, 1H), 7.05 – 6.99 (m, 4H), 6.32 – 6.07 (m, 2H), 5.67 – 5.58 (m, 2H), 5.42 (d, J = 2.5 Hz, 1H), 5.10 (d, J = 2.1 Hz, 1H), 4.56 (dd, J = 11.4, 8.3 Hz, 1H), 3.87 (dd, J = 11.4, 5.7 Hz, 1H). ^{13}C NMR (126 MHz, $CDCl_3$ + CD_3OD) δ 165.74, 157.06, 156.46, 155.68, 150.38, 145.43, 137.59, 133.07, 130.61 (2C), 129.48, 129.38 (2C), 126.90, 126.68, 123.49, 119.02 (2C), 118.15 (2C), 108.34, 108.21, 105.37, 54.08, 47.55. MS (ESI, $[M + H]^+$) m/z 424.3. HRMS (ESI) calcd for $C_{25}H_{22}N_5O_2$, 424.1768; found, 424.1765.

(*R*)-*N*-(4-Amino-6-methylene-5-(4-phenoxyphenyl)-7,8-dihydro-6*H*-pyrimido [5,4-*b*]pyrrolizin-7-yl)acrylamide (7R). White solid. Yield 203 mg, 48.0%. ^{1}H NMR (300 MHz, $CDCl_3$) δ 8.24 (s, 1H), 7.45 (d, J = 8.7 Hz, 2H), 7.43 – 7.36 (m, 2H), 7.17 (t, J = 7.4 Hz, 1H), 7.10 (d, J = 8.4 Hz, 4H), 6.44 – 6.10 (m, 3H), 5.80 – 5.64 (m, 2H), 5.51 (d, J = 2.1 Hz, 1H), 5.18 (d, J = 1.9 Hz, 1H), 5.04 (s, 2H), 4.67 (dd, J = 11.5, 8.1 Hz, 1H), 3.98 (dd, J = 11.6, 4.8 Hz, 1H). ^{13}C NMR (126 MHz, $CDCl_3$) δ 165.99, 157.52, 157.10, 156.21, 151.22, 146.02, 138.25, 133.36, 131.14 (2C), 130.07, 129.93 (2C), 127.53, 127.28, 124.02, 119.57 (2C), 118.66 (2C), 108.80, 108.72, 105.85, 54.62, 48.26. MS (ESI, $[M + H]^+$) m/z 424.3. HRMS (ESI) calcd for $C_{25}H_{22}N_5O_2$, 424.1768; found, 424.1762. $[\alpha]^{20}_D$ +107.3 (c 0.05, MeOH).

(*S*)-*N*-(4-Amino-6-methylene-5-(4-phenoxyphenyl)-7,8-dihydro-6*H*-pyrimido [5,4-*b*]pyrrolizin-7-yl)acrylamide (7S). White solid. Yield 184 mg, 43.5%. ^{1}H NMR

(300 MHz, $CDCl_3$) δ 8.23 (s, 1H), 7.50 – 7.35 (m, 4H), 7.17 (t, *J* = 7.4 Hz, 1H), 7.10 (d, *J* = 8.3 Hz, 4H), 6.45 – 6.11 (m, 3H), 5.74 (d, *J* = 10.2 Hz, 1H), 5.72 – 5.64 (m, 1H), 5.51 (d, *J* = 2.0 Hz, 1H), 5.18 (d, *J* = 1.7 Hz, 1H), 5.10 (s, 2H), 4.66 (dd, *J* = 11.6, 8.0 Hz, 1H), 3.98 (dd, *J* = 11.6, 4.8 Hz, 1H). ^{13}C NMR (126 MHz, $CDCl_3$) δ 165.34, 157.54, 157.11, 156.30, 152.21, 146.89, 138.54, 132.95, 131.21 (2C), 130.02, 129.99 (2C), 127.92, 127.59, 124.07, 119.64 (2C), 118.71 (2C), 108.84, 108.69, 106.20, 55.11, 49.10. MS (ESI, $[M + H]^+$) m/z 424.4. HRMS (ESI) calcd for $C_{25}H_{22}N_5O_2$, 424.1768; found, 424.1771. $[\alpha]^{20}_D$ -106.0 (c 0.05, MeOH).

General Procedure for Synthesis of Compound 8-13, 15. To a solution of intermediate **14** in CH_2Cl_2 (25 mL) was added corresponding R^4-COOH (1.1 mmol), HATU (418 mg, 1.1 mmol) and Et_3N (0.28 mL, 2.0 mmol) dropwise at 0 ^oC. The mixture was stirred at room temperature for 1.5 h. After completion, the mixture was diluted with water (10 mL) and extracted with CH_2Cl_2 (3 × 5 mL). The combined organic phase was washed with brine (5 mL), dried over Na_2SO_4, filtered, and concentrated in vacuo. The residue was purified by silica column chromatography ($CHCl_3$/MeOH) to give compound **8-13** and **15**.

***N*-(2-((4-Amino-6-methylene-5-(4-phenoxyphenyl)-7,8-dihydro-6*H*-pyrimido [5,4-*b*]pyrrolizin-7-yl)amino)-2-oxoethyl)acrylamide (8).** White solid. Yield 418 mg, 87.0%. ^{1}H NMR (300 MHz, $CDCl_3$ + CD_3OD) *δ* 8.08 (s, 1H), 7.37 (d, *J* = 8.7 Hz, 2H), 7.32 (dd, *J* = 8.4, 7.6 Hz, 2H), 7.10 (t, *J* = 7.4 Hz, 1H), 7.06 – 6.98 (m, 4H), 6.26 – 6.07 (m, 2H), 5.62 (dd, *J* = 9.5, 2.2 Hz, 1H), 5.54 – 5.45 (m, 1H), 5.41 (d, *J* = 2.4 Hz, 1H), 5.08 (d, *J* = 2.1 Hz, 1H), 4.54 (dd, *J* = 11.4, 8.4 Hz, 1H), 3.91 (s, 2H), 3.84 (dd, *J* = 11.4, 5.7 Hz, 1H). ^{13}C NMR (126 MHz, $CDCl_3$ + CD_3OD) *δ* 169.02, 166.21, 157.06, 156.53, 155.70, 150.55, 145.48, 137.22, 132.86, 130.61 (2C), 129.39 (2C), 129.35, 126.79, 126.70, 123.49, 119.03 (2C), 118.15 (2C), 109.50, 108.36, 108.16,

105.39, 54.15, 47.54, 42.26. MS (ESI, [M + H]$^+$) m/z 481.2. HRMS (ESI) calcd for $C_{27}H_{25}N_6O_3$, 481.1983; found, 481.1983.

***N*-((2*S*)-1-((4-Amino-6-methylene-5-(4-phenoxyphenyl)-7,8-dihydro-6*H*-pyrimido[5,4-*b*]pyrrolizin-7-yl)amino)-1-oxopropan-2-yl)acrylamide (9).** White solid. Yield 392 mg, 79.3%. ^{1}H NMR (300 MHz, $CDCl_3$ + CD_3OD) δ 8.11 (s, 0.5H), 8.10 (s, 0.5H), 7.41 – 7.30 (m, 4H), 7.11 (t, J = 7.4 Hz, 1H), 7.04 (dd, J = 8.4, 1.7 Hz, 4H), 6.27 – 6.05 (m, 2H), 5.65 – 5.59 (m, 1H), 5.53 – 5.45 (m, 1H), 5.42 (s, 1H), 5.06 (s, 1H), 4.57 (ddd, J = 11.5, 8.4, 2.9 Hz, 1H), 4.51 – 4.40 (m, 1H), 3.85 (dt, J = 11.5, 5.6 Hz, 1H), 1.34 (dd, J = 6.9, 5.0 Hz, 3H). ^{13}C NMR (151 MHz, $CDCl_3$ + CD_3OD) δ 173.07 (0.5C), 172.96 (0.5C), 166.00 (0.5C), 165.94 (0.5C), 157.58, 156.97, 156.21, 151.01, 146.02, 137.63, 133.44 (0.5C), 133.40 (0.5C), 131.15 (2C), 130.01, 129.94 (2C), 127.39 (0.5C), 127.34 (0.5C), 127.22, 124.04, 119.58 (2C), 118.68 (2C), 108.90 (0.5C), 108.84 (0.5C), 108.76 (0.5C), 108.52 (0.5C), 105.90, 54.65 (0.5C), 54.54 (0.5C), 48.60, 48.07, 18.01 (0.5C), 17.73 (0.5C). MS (ESI, [M + H]$^+$) m/z 495.3. HRMS (ESI) calcd for $C_{28}H_{27}N_6O_3$, 495.2139; found, 495.2145.

1-Acrylamido-*N*-(4-amino-6-methylene-5-(4-phenoxyphenyl)-7,8-dihydro-6*H*-pyrimido[5,4-*b*]pyrrolizin-7-yl)cyclopropanecarboxamide (10). White solid. Yield 332 mg, 65.5%. ^{1}H NMR (300 MHz, $CDCl_3$ + CD_3OD) δ 8.08 (s, 1H), 7.41 – 7.32 (m, 4H), 7.12 (t, J = 7.4 Hz, 1H), 7.04 (d, J = 8.5 Hz, 4H), 6.28 – 5.99 (m, 2H), 5.60 (dd, J = 10.2, 1.4 Hz, 1H), 5.57 – 5.50 (m, 1H), 5.42 (d, J = 2.5 Hz, 1H), 5.13 (d, J = 2.1 Hz, 1H), 4.58 (dd, J = 11.3, 8.6 Hz, 1H), 3.83 (dd, J = 11.4, 6.1 Hz, 1H), 1.65 – 1.45 (m, 2H), 1.09 – 0.96 (m, 2H). ^{13}C NMR (126 MHz, $CDCl_3$ + CD_3OD) δ 172.30, 167.51, 157.51, 157.10, 156.26, 151.24, 146.01, 138.10, 133.42, 131.17 (2C), 129.93 (2C), 127.69, 127.34, 123.99, 119.55 (2C), 118.69 (2C), 108.67, 108.51, 105.91, 77.29, 54.80, 48.16, 34.94, 17.08, 16.91. MS (ESI, [M + H]$^+$) m/z 507.3. HRMS (ESI)

calcd for $C_{29}H_{27}N_6O_3$, 507.2139; found, 507.2147.

***N*-(3-((4-Amino-6-methylene-5-(4-phenoxyphenyl)-7,8-dihydro-6*H*-pyrimido[5,4-*b*]pyrrolizin-7-yl)amino)-3-oxopropyl)acrylamide (11).** White solid. Yield 448 mg, 90.6%. ^{1}H NMR (300 MHz, $CDCl_3$ + CD_3OD) δ 8.09 (s, 1H), 7.37 (d, J = 8.6 Hz, 2H), 7.35 – 7.29 (m, 2H), 7.10 (t, J = 7.4 Hz, 1H), 7.02 (d, J = 8.6 Hz, 4H), 6.21 – 5.98 (m, 2H), 5.55 (dd, J = 9.9, 1.9 Hz, 1H), 5.52 – 5.43 (m, 1H), 5.40 (d, J = 2.3 Hz, 1H), 5.04 (d, J = 2.0 Hz, 1H), 4.53 (dd, J = 11.3, 8.2 Hz, 1H), 3.81 (dd, J = 11.4, 5.7 Hz, 1H), 2.43 (t, J = 6.4 Hz, 2H). ^{13}C NMR (151 MHz, $CDCl_3$ + CD_3OD) δ 172.26, 166.81, 157.53, 157.16, 156.18, 151.23, 145.98, 137.86, 133.39, 131.13 (2C), 130.35, 129.92 (2C), 127.27, 126.69, 124.02, 119.56 (2C), 118.64 (2C), 108.79, 108.49, 105.93, 54.67, 48.18, 35.80, 35.30. MS (ESI, $[M + H]^+$) m/z 495.4. HRMS (ESI) calcd for $C_{28}H_{27}N_6O_3$, 495.2139; found, 495.2140.

(*E*)-*N*-(4-Amino-6-methylene-5-(4-phenoxyphenyl)-7,8-dihydro-6*H*-pyrimido[5,4-*b*]pyrrolizin-7-yl)-4-(dimethylamino)but-2-enamide (12). White solid. Yield 333 mg, 69.3%. ^{1}H NMR (300 MHz, $CDCl_3$) δ 8.25 (s, 1H), 7.47 (d, J = 8.5 Hz, 2H), 7.40 (t, J = 7.9 Hz, 2H), 7.20 – 7.15 (m, 1H), 7.11 (d, J = 8.6 Hz, 4H), 6.92 (dt, J = 15.0, 6.0 Hz, 1H), 6.14 – 6.00 (m, 2H), 5.76 – 5.61 (m, 1H), 5.51 (d, J = 1.9 Hz, 1H), 5.17 (d, J = 1.7 Hz, 1H), 5.04 (s, 2H), 4.69 (dd, J = 11.7, 7.9 Hz, 1H), 3.97 (dd, J = 11.6, 4.8 Hz, 1H), 3.12 (dd, J = 5.7, 0.7 Hz, 2H), 2.30 (s, 6H). ^{13}C NMR (151 MHz, $CDCl_3$) δ 165.31, 157.52, 157.19, 156.32, 152.36, 146.93, 142.25, 138.65, 132.93, 131.24 (2C), 130.00 (2C), 127.68, 124.79, 124.06, 119.65 (2C), 118.72 (2C), 108.79, 108.53, 106.24, 60.25, 55.07, 49.05, 45.48. ^{13}C NMR (151 MHz, $CDCl_3$) δ 165.31, 157.52, 157.19, 156.32, 152.36, 146.93, 142.25, 138.65, 132.93, 131.24 (2C), 130.00 (2C), 127.68, 124.79, 124.06, 119.65 (2C), 118.72 (2C), 108.79, 108.53, 106.24, 60.25, 55.07, 49.05, 45.48. MS (ESI, $[M + H]^+$) m/z 481.3. HRMS (ESI) calcd for

$C_{28}H_{29}N_6O_2$, 481.2347; found, 481.2334.

Compounds **13R** and **13S** were prepared following the synthetic procedure for racemate **13** from their corresponding enantiomeric precursors.

***N*-(4-Amino-6-methylene-5-(4-phenoxyphenyl)-7,8-dihydro-6*H*-pyrimido[5,4-*b*]pyrrolizin-7-yl)but-2-ynamide (13).** White solid. Yield 381 mg, 87.5%. ^{1}H NMR (300 MHz, $CDCl_3$) δ 8.24 (s, 1H), 7.46 (d, J = 8.6 Hz, 2H), 7.40 (t, J = 8.0 Hz, 2H), 7.18 (t, J = 7.4 Hz, 1H), 7.14 – 7.07 (m, 4H), 6.30 (d, J = 8.4 Hz, 1H), 5.68 – 5.57 (m, 1H), 5.53 (d, J = 2.0 Hz, 1H), 5.21 (d, J = 1.4 Hz, 1H), 5.16 (s, 2H), 4.67 (dd, J = 11.7, 7.9 Hz, 1H), 3.98 (dd, J = 11.7, 5.0 Hz, 1H), 1.97 (s, 3H). ^{13}C NMR (126 MHz, $CDCl_3$) δ 157.60, 157.02, 156.29, 153.25, 152.02, 146.85, 137.94, 132.79, 131.20 (2C), 130.00 (2C), 127.50, 124.08, 119.66 (2C), 118.74 (2C), 108.99, 108.93, 106.19, 85.12, 74.32, 55.18, 48.82, 3.74. MS (ESI, $[M + H]^+$) m/z 436.3. HRMS (ESI) calcd for $C_{26}H_{22}N_5O_2$, 436.1768; found, 436.1757.

(*R*)-*N*-(4-amino-6-methylene-5-(4-phenoxyphenyl)-7,8-dihydro-6*H*-pyrimido[5,4-*b*]pyrrolizin-7-yl)but-2-ynamide (13R). White solid. Yield 390 mg, 89.6%. ^{1}H NMR (300 MHz, $CDCl_3$) δ 8.22 (s, 1H), 7.47 – 7.36 (m, 4H), 7.17 (t, J = 7.4 Hz, 1H), 7.10 (d, J = 8.4 Hz, 4H), 6.44 (d, J = 8.2 Hz, 1H), 5.69 – 5.57 (m, 1H), 5.52 (s, 1H), 5.20 (s, 3H), 4.65 (dd, J = 11.6, 8.0 Hz, 1H), 3.97 (dd, J = 11.5, 4.9 Hz, 1H), 1.95 (s, 3H). ^{13}C NMR (126 MHz, $CDCl_3$) δ 157.54, 157.25, 156.32, 153.26, 152.34, 146.92, 137.99, 132.69, 131.20 (2C), 129.98 (2C), 127.59, 124.05, 119.63 (2C), 118.72 (2C), 108.92, 108.77, 106.23, 85.07, 74.33, 55.19, 48.78, 3.71. MS (ESI, $[M + H]^+$) m/z 436.4. HRMS (ESI) calcd for $C_{26}H_{22}N_5O_2$, 436.1768; found, 436.1767. $[\alpha]^{20}_D$ +134.0 (c 0.05, MeOH).

(*S*)-*N*-(4-Amino-6-methylene-5-(4-phenoxyphenyl)-7,8-dihydro-6*H*-pyrimido[5,4-*b*]pyrrolizin-7-yl)but-2-ynamide (13S). White solid. Yield 365 mg, 83.8%. ^{1}H

NMR (300 MHz, $CDCl_3$) δ 8.25 (s, 1H), 7.45 (d, J = 8.6 Hz, 2H), 7.43 – 7.36 (m, 2H), 7.21 – 7.15 (m, 1H), 7.10 (d, J = 8.6 Hz, 4H), 6.33 (d, J = 8.1 Hz, 1H), 5.69 – 5.57 (m, 1H), 5.52 (d, J = 2.1 Hz, 1H), 5.20 (d, J = 1.6 Hz, 1H), 5.09 (s, 2H), 4.66 (dd, J = 11.6, 8.0 Hz, 1H), 3.97 (dd, J = 11.6, 4.9 Hz, 1H), 1.96 (s, 3H). ^{13}C NMR (126 MHz, $CDCl_3$) δ 157.55, 157.23, 156.31, 153.26, 152.57, 152.45, 146.98, 137.98, 132.66, 131.21 (2C), 129.99 (2C), 127.61, 124.06, 119.64 (2C), 118.72 (2C), 108.91, 108.77, 106.26, 85.10, 74.31, 55.20, 48.80, 3.74. MS (ESI, $[M + H]^+$) m/z 436.3. HRMS (ESI) calcd for $C_{26}H_{22}N_5O_2$, 436.1768; found, 436.1780. $[\alpha]^{20}_D$ -150.0 (c 0.05, MeOH).

6-Methylene-5-(4-phenoxyphenyl)-7,8-dihydro-6*H*-pyrimido[5,4-*b*]pyrrolizine-4,7-diamine (14). To a solution of intermediate **33** (470 mg, 1.0 mmol) in CH_2Cl_2 (20 mL) was added trifluoroacetic acid (1.9 mL) dropwise. The mixture was stirred at room temperature for 3 h. After completion, the mixture was added saturated $NaHCO_3$ solution dropwise until neutral and then extracted with CH_2Cl_2 (3 × 5 mL). The combined organic phase was washed with brine (5 mL), dried over Na_2SO_4, filtered, and concentrated in vacuo. The crude product **14** (362 mg, 98.0%) was given as yellowish solid and could be used in next step without further purification. ^{1}H NMR (300 MHz, $CDCl_3$) δ 8.23 (s, 1H), 7.47 (d, J = 8.5 Hz, 2H), 7.40 (t, J = 7.9 Hz, 2H), 7.17 (t, J = 7.4 Hz, 1H), 7.10 (d, J = 8.5 Hz, 4H), 5.49 (d, J = 1.6 Hz, 1H), 5.43 (s, 2H), 5.19 (s, 1H), 4.68 – 4.50 (m, 2H), 3.81 (dd, J = 9.7, 4.4 Hz, 1H). ^{13}C NMR (126 MHz, CD_3OD) δ 153.36, 153.23, 152.51, 148.20, 143.00, 139.19, 129.83, 127.35 (2C), 126.01 (2C), 124.19, 120.00, 115.61 (2C), 114.78 (2C), 104.37, 103.01, 102.11, 54.42, 46.98. MS (ESI, $[M + H]^+$) m/z 370.3. HRMS (ESI) calcd for $C_{22}H_{20}N_5O$, 370.1662; found, 370.1652.

***N*-(4-Amino-6-methylene-5-(4-phenoxyphenyl)-7,8-dihydro-6*H*-pyrimido[5,4-*b*]pyrrolizin-7-yl)propionamide (15).** White solid. Yield 314 mg, 73.8%. ^{1}H NMR

(300 MHz, $CDCl_3$ + CD_3OD) δ 8.06 (s, 1H), 7.36 (d, J = 8.5 Hz, 2H), 7.31 (t, J = 7.9 Hz, 2H), 7.08 (t, J = 7.5 Hz, 1H), 7.01 (d, J = 8.3 Hz, 4H), 5.57 – 5.48 (m, 1H), 5.39 (s, 1H), 5.05 (s, 1H), 4.51 (dd, J = 11.4, 8.4 Hz, 1H), 3.80 (dd, J = 11.4, 5.8 Hz, 1H), 2.19 (q, J = 7.7 Hz, 2H), 1.09 (t, J = 7.6 Hz, 3H). ^{13}C NMR (126 MHz, $CDCl_3$ + CD_3OD) δ 179.00, 161.49, 161.17, 160.18, 155.28, 149.97, 142.34, 137.44, 135.10 (2C), 133.85 (2C), 131.27, 127.95, 123.48 (2C), 122.61 (2C), 112.69, 112.33, 109.91, 58.55, 58.43, 52.15, 52.11, 33.21, 33.16, 13.60. MS (ESI, $[M + H]^+$) m/z 426.3. HRMS (ESI) calcd for $C_{25}H_{24}N_5O_2$, 426.1925; found, 426.1926.

Compounds **16-19** were prepared following the synthetic procedure of compound **7** staring from intermediates **36a-d**.

(*S*)-*N*-(4-Amino-5-(4-(4-(*tert*-butyl)phenoxy)phenyl)-6-methylene-7,8-dihydro-6*H*-pyrimido[5,4-*b*]pyrrolizin-7-yl)acrylamide (16). White solid. Yield 354 mg, 73.8%. ^{1}H NMR (300 MHz, $CDCl_3$) δ 8.20 (s, 1H), 7.40 (dd, J = 8.7, 3.0 Hz, 4H), 7.05 (dd, J = 16.2, 8.6 Hz, 4H), 6.62 (d, J = 8.1 Hz, 1H), 6.46 – 6.12 (m, 2H), 5.73 (d, J = 10.3 Hz, 2H), 5.54 – 5.45 (m, 1H), 5.17 (s, 1H), 5.15 (s, 2H), 4.63 (dd, J = 11.5, 8.0 Hz, 1H), 3.97 (dd, J = 11.5, 4.6 Hz, 1H), 1.34 (s, 9H). ^{13}C NMR (126 MHz, $CDCl_3$) δ 165.37, 157.90, 157.08, 153.73, 152.05, 147.06, 146.78, 138.53, 132.99, 131.12 (2C), 130.09, 127.82, 127.19, 126.79 (2C), 119.22 (2C), 118.42 (2C), 108.93, 108.73, 106.16, 55.10, 49.09, 34.42, 31.50 (3C). MS (ESI, $[M + H]^+$) m/z 480.4. HRMS (ESI) calcd for $C_{29}H_{30}N_5O_2$, 480.2394; found, 480.2403. $[\alpha]^{20}_D$ -92.0 (c 0.05, MeOH).

(*S*)-*N*-(4-Amino-5-(4-(4-fluorophenoxy)phenyl)-6-methylene-7,8-dihydro-6*H*-pyrimido[5,4-*b*]pyrrolizin-7-yl)acrylamide (17). White solid. Yield 286 mg, 64.8%. ^{1}H NMR (300 MHz, $CDCl_3$) δ 8.20 (s, 1H), 7.43 (d, J = 8.4 Hz, 2H), 7.11 – 7.00 (m, 6H), 6.48 (d, J = 7.9 Hz, 1H), 6.44 – 6.12 (m, 2H), 5.78 – 5.64 (m, 2H), 5.51 (s, 1H),

5.23 (s, 2H), 5.19 (s, 1H), 4.66 (dd, *J* = 11.5, 8.0 Hz, 1H), 3.99 (dd, *J* = 11.8, 4.8 Hz, 1H). ^{13}C NMR (126 MHz, $CDCl_3$) δ 165.36, 160.25, 158.32, 157.95, 156.82, 151.90, 151.59, 146.71, 138.49, 133.17, 131.23 (2C), 130.03, 127.90, 127.41, 121.37, 121.31, 118.15 (2C), 116.70, 116.51, 108.85, 106.06, 55.08, 49.09. MS (ESI, $[M + H]^+$) m/z 442.3. HRMS (ESI) calcd for $C_{25}H_{21}FN_5O_2$, 442.1674; found, 442.1681. $[\alpha]^{20}_D$ -109.3 (c 0.05, MeOH).

(*S*)-*N*-(4-Amino-6-methylene-5-(4-(4-(trifluoromethyl)phenoxy)phenyl)-7,8-dihydro-6*H*-pyrimido[5,4-*b*]pyrrolizin-7-yl)acrylamide (18). White solid. Yield 377 mg, 76.7%. ^{1}H NMR (300 MHz, $CDCl_3$ + CD_3OD) δ 8.18 (s, 1H), 7.63 (d, *J* = 8.5 Hz, 2H), 7.50 (d, *J* = 8.4 Hz, 2H), 7.14 (d, *J* = 8.2 Hz, 4H), 6.68 (d, *J* = 8.5 Hz, 1H), 6.45 – 6.11 (m, 2H), 5.79 – 5.65 (m, 2H), 5.50 (d, *J* = 1.5 Hz, 1H), 5.33 (s, 2H), 5.20 (d, *J* = 0.9 Hz, 1H), 4.64 (dd, *J* = 11.5, 8.0 Hz, 1H), 3.98 (dd, *J* = 11.6, 4.8 Hz, 1H). ^{13}C NMR (126 MHz, $CDCl_3$) δ 165.43, 159.57, 157.05, 156.00, 151.87, 146.70, 138.51, 133.20, 131.51 (2C), 130.03, 128.92, 127.91, 127.37, 127.35, 126.12, 125.87, 125.60, 125.34, 125.15, 122.99, 119.84 (2C), 118.70 (2C), 108.87, 108.57, 106.01, 55.06, 50.74, 49.02. MS (ESI, $[M + H]^+$) m/z 492.3. HRMS (ESI) calcd for $C_{26}H_{21}F_3N_5O_2$, 492.1642; found, 492.1649. $[\alpha]^{20}_D$ -86.0 (c 0.05, MeOH).

(*S*)-*N*-(4-Amino-6-methylene-5-(4-(4-(trifluoromethoxy)phenoxy)phenyl)-7,8-dihydro-6*H*-pyrimido[5,4-*b*]pyrrolizin-7-yl)acrylamide (19). White solid. Yield 345 mg, 68.0%. ^{1}H NMR (300 MHz, $CDCl_3$) δ 8.21 (s, 1H), 7.47 (d, *J* = 8.3 Hz, 2H), 7.24 (d, *J* = 8.8 Hz, 2H), 7.10 (d, *J* = 7.6 Hz, 4H), 6.47 (d, *J* = 8.2 Hz, 1H), 6.44 – 6.10 (m, 2H), 5.79 – 5.65 (m, 2H), 5.51 (d, *J* = 1.8 Hz, 1H), 5.27 (s, 2H), 5.19 (d, *J* = 0.9 Hz, 1H), 4.66 (dd, *J* = 11.6, 8.0 Hz, 1H), 3.99 (dd, *J* = 11.6, 4.9 Hz, 1H). ^{13}C NMR (126 MHz, $CDCl_3$) δ 165.36, 157.05, 156.94, 154.86, 151.76, 146.77, 145.09, 138.52, 133.16, 131.37 (2C), 130.01, 128.15, 127.93, 122.80 (2C), 120.43 (2C),

118.94 (2C), 108.83, 108.72, 106.06, 55.09, 49.09. MS (ESI, $[M + H]^+$) m/z 508.3. HRMS (ESI) calcd for $C_{26}H_{21}F_3N_5O_3$, 508.1591; found, 508.1605. $[\alpha]^{20}_D$ -82.0 (c 0.05, MeOH).

General Procedure for Synthesis of Compound 20-24. To a solution of compound **37e-i** (1.0 mmol) in THF (15 mL) was added $PdCl_2$dppf (76 mg, 0.1 mmol). 4N NaOH aqueous solution (3 mL, 12.0 mmol) was added and the mixture was stirred at 85 ^oC for 15 h under N_2. After completion, the mixture was diluted with water (10 mL) and extracted with ethyl acetate (3 × 5 mL). The combined organic phase was washed with brine (5 mL), dried over Na_2SO_4, filtered, and concentrated in vacuo. The residue was purified by silica column chromatography ($CHCl_3$/MeOH) to give compound **38e-i** as yellowish solid. Compounds **20-24** were prepared following the synthetic procedure of compound **7** staring from intermediates **38e-i**.

(*S*)-4-(7-Acrylamido-4-amino-6-methylene-7,8-dihydro-6*H*-pyrimido[5,4-*b*]pyrrolizin-5-yl)-*N*-(pyridin-2-yl)benzamide (20). White solid. Yield 248 mg, 55.0%. ^1H NMR (300 MHz, $CDCl_3$) δ 8.89 (s, 1H), 8.39 (d, J = 8.4 Hz, 1H), 8.31 (d, J = 5.0 Hz, 1H), 8.21 (s, 1H), 8.02 (d, J = 8.0 Hz, 2H), 7.78 (t, J = 7.8 Hz, 1H), 7.63 (d, J = 8.1 Hz, 2H), 7.16 – 7.05 (m, 1H), 6.50 (d, J = 7.6 Hz, 1H), 6.45 – 6.11 (m, 2H), 5.82 – 5.66 (m, 2H), 5.49 (s, 1H), 5.18 (s, 3H), 4.68 (dd, J = 11.6, 8.1 Hz, 1H), 3.99 (dd, J = 11.6, 4.9 Hz, 1H). ^{13}C NMR (151 MHz, $CDCl_3$) δ 220.96, 165.44, 165.25, 157.18, 152.60, 151.44, 148.00, 147.24, 138.64, 138.42, 137.71, 133.64, 133.32, 130.26 (2C), 129.98, 128.09, 128.06 (2C), 120.23, 114.31, 109.19, 108.22, 105.79, 55.01, 49.03. MS (ESI, $[M + H]^+$) m/z 452.2. HRMS (ESI) calcd for $C_{25}H_{22}N_7O_2$, 452.1829; found, 452.1838. $[\alpha]^{20}_D$ -97.3 (c 0.05, MeOH).

(*S*)-4-(7-Acrylamido-4-amino-6-methylene-7,8-dihydro-6*H*-pyrimido[5,4-*b*]pyrrolizin-5-yl)-*N*-(4-(trifluoromethyl)pyridin-2-yl)benzamide (21). White solid.

Yield 276 mg, 61.1%. ^{1}H NMR (300 MHz, $CDCl_3$) δ 8.66 (s, 1H), 8.44 (d, J = 5.1 Hz, 1H), 8.13 (s, 1H), 8.05 (d, J = 8.3 Hz, 2H), 7.70 (d, J = 8.2 Hz, 1H), 7.63 (d, J = 8.3 Hz, 2H), 7.28 (d, J = 4.7 Hz, 1H), 6.36 – 6.10 (m, 2H), 5.67 (d, J = 8.7 Hz, 2H), 5.46 (d, J = 2.0 Hz, 1H), 5.16 (d, J = 1.4 Hz, 1H), 4.60 (dd, J = 11.4, 8.5 Hz, 1H), 3.93 (dd, J = 11.5, 5.6 Hz, 1H). ^{13}C NMR (126 MHz, $CDCl_3$ + CD_3OD) δ 166.11, 165.65, 156.86, 152.52, 151.28, 148.92, 146.46, 141.15, 140.88, 140.61, 140.34, 138.11, 137.74, 133.94, 132.94, 130.21 (2C), 129.96, 128.28 (2C), 127.61, 125.87, 123.69, 121.52, 119.35, 115.64, 115.61, 110.56, 110.53, 109.26, 108.23, 105.47, 54.62, 48.19. MS (ESI, $[M - H]^-$) m/z 518.3. HRMS (ESI) calcd for $C_{26}H_{19}F_3N_7O_2$, 518.1558; found, 518.1567. $[\alpha]^{20}_D$ -84.0 (c 0.05, MeOH).

4-((*S*)-7-Acrylamido-4-amino-6-methylene-7,8-dihydro-6*H*-pyrimido[5,4-*b*]pyrrolizin-5-yl)-*N*-((*S*)-1-(pyridin-2-yl)ethyl)benzamide (22). White solid. Yield 304 mg, 63.4%. ^{1}H NMR (300 MHz, $CDCl_3$) δ 8.58 (d, J = 4.7 Hz, 1H), 8.20 (s, 1H), 8.01 (d, J = 7.1 Hz, 1H), 7.96 (d, J = 8.1 Hz, 2H), 7.71 (t, J = 7.7 Hz, 1H), 7.55 (d, J = 7.9 Hz, 2H), 7.32 (d, J = 7.9 Hz, 1H), 7.23 (d, J = 7.4 Hz, 1H), 6.58 (d, J = 7.2 Hz, 1H), 6.45 – 6.14 (m, 2H), 5.80 – 5.68 (m, 2H), 5.49 (s, 1H), 5.44 – 5.28 (m, 3H), 5.18 (s, 1H), 4.68 (dd, J = 11.5, 8.2 Hz, 1H), 4.02 (dd, J = 11.9, 5.0 Hz, 1H), 1.60 (d, J = 6.7 Hz, 3H). ^{13}C NMR (126 MHz, $CDCl_3$) δ 165.92, 165.44, 160.72, 156.52, 151.16, 149.01, 146.83, 138.31, 137.09, 136.38, 134.28, 133.56, 130.03, 129.87 (2C), 127.99 (2C), 127.94, 122.56, 121.66, 109.41, 108.72, 105.65, 54.97, 50.20, 49.08, 22.98. MS (ESI, $[M + H]^+$) m/z 480.3. HRMS (ESI) calcd for $C_{27}H_{26}N_7O_2$, 480.2142; found, 480.2147. $[\alpha]^{20}_D$ -41.3 (c 0.05, MeOH).

(*S*)-4-(7-Acrylamido-4-amino-6-methylene-7,8-dihydro-6*H*-pyrimido[5,4-*b*]pyrrolizin-5-yl)-*N*-benzylbenzamide (23). White solid. Yield 358 mg, 79.3%. ^{1}H NMR (300 MHz, $CDCl_3$ + CD_3OD) δ 8.03 (s, 1H), 7.82 (d, J = 8.3 Hz, 2H), 7.44 (d, J

= 8.2 Hz, 2H), 7.27 – 7.21 (m, 4H), 7.21 – 7.15 (m, 1H), 6.29 – 6.05 (m, 2H), 5.60 (dd, *J* = 10.0, 1.7 Hz, 1H), 5.58 – 5.52 (m, 1H), 5.34 (d, *J* = 2.3 Hz, 1H), 5.04 (d, *J* = 1.9 Hz, 1H), 4.53 (s, 2H), 4.52 – 4.45 (m, 1H), 3.83 (dd, *J* = 11.4, 5.7 Hz, 1H). ^{13}C NMR (126 MHz, $CDCl_3$ + CD_3OD) δ 167.43, 167.36, 166.17, 157.06, 151.49, 146.33, 138.10, 136.59, 133.63, 130.00, 129.85 (2C), 128.65 (2C), 127.92 (2C), 127.73 (2C), 127.49 (2C), 108.95, 108.34, 105.52, 54.56, 48.07, 44.06, 43.93. (ESI, $[M + H]^+$) m/z 465.2. HRMS (ESI) calcd for $C_{27}H_{25}N_6O_2$, 465.2034; found, 465.2041. $[\alpha]^{20}_D$ -82.0 (c 0.05, MeOH).

4-((*S*)-7-Acrylamido-4-amino-6-methylene-7,8-dihydro-6*H*-pyrimido[5,4-*b*]pyrrolizin-5-yl)-*N*-((*R*)-2-methoxy-1-phenylethyl)benzamide (24). White solid. Yield 202 mg, 44.7%. ^{1}H NMR (300 MHz, $CDCl_3$ + CD_3OD) δ 8.15 (s, 1H), 7.87 (d, *J* = 8.2 Hz, 2H), 7.52 (d, *J* = 8.2 Hz, 2H), 7.37 – 7.22 (m, 6H), 6.36 – 6.03 (m, 2H), 5.70 – 5.60 (m, 2H), 5.42 (d, *J* = 2.3 Hz, 1H), 5.31 (t, *J* = 5.0 Hz, 1H), 5.11 (d, *J* = 1.8 Hz, 1H), 4.60 (dd, *J* = 11.5, 8.1 Hz, 1H), 3.90 (dd, *J* = 11.6, 5.5 Hz, 1H), 3.73 (d, *J* = 4.8 Hz, 2H), 3.34 (s, 3H). ^{13}C NMR (126 MHz, $CDCl_3$ + CD_3OD) δ 166.52, 165.68, 157.09, 152.09, 146.82, 139.59, 138.30, 136.90, 133.71, 133.44, 130.00 (2C), 129.95, 128.64 (2C), 127.96 (2C), 127.80, 127.66, 126.78 (2C), 109.08, 108.38, 105.78, 74.90, 59.13, 54.75, 53.05, 48.59. MS (ESI, $[M - H]^-$) m/z 507.4. HRMS (ESI) calcd for $C_{29}H_{27}N_6O_3$, 507.2150; found, 507.2159. $[\alpha]^{20}_D$ -43.7 (c 0.05, MeOH).

2-((*tert*-Butoxycarbonyl)amino)but-3-en-1-yl methanesulfonate (26). To a solution of compound **25** (1.87 g, 10.0 mmol) in CH_2Cl_2 (20 mL) was added methanesulfonyl chloride (0.85 mL, 11.0 mmol) and triethylamine (1.7 mL, 12.0 mmol) dropwise at 0 ^{o}C. The mixture was allowed to warm to room temperature slowly for 3 h. After completion of the reaction, water (20 mL) and CH_2Cl_2 (20 mL) were added. The organic phase was separated, dried over Na_2SO_4, filtered, and

concentrated in vacuo. The residue was purified by silica column chromatography (petroleum ether/EtOAc) to give compound **26** (2.27 g, 85.4%) as white solid. ^{1}H NMR (300 MHz, $CDCl_3$) δ 5.78 (ddd, J = 15.8, 10.2, 5.2 Hz, 1H), 5.39 – 5.15 (m, 2H), 4.91 (d, J = 6.9 Hz, 1H), 4.43 (s, 1H), 4.32 – 4.12 (m, 2H), 3.00 (s, 3H), 1.42 (s, 9H).

***tert*-Butyl (1-(4-chloro-5-iodo-7*H*-pyrrolo[2,3-*d*]pyrimidin-7-yl)but-3-en-2-yl) carbamate (27).** To a solution of 4-chloro-5-iodo-7*H*-pyrrolo[2,3-*d*]pyrimidine (279 mg, 1.0 mmol) in dry DMF (7 mL) was added K_2CO_3 (276 mg, 2.0 mmol) and compound **26** (398 mg, 1.5 mmol). The mixture was stirred at 55 ^{o}C for 12 h under N_2. After completion of the reaction, the mixture was diluted with water (10 mL) and extracted with ethyl acetate (3 × 5 mL). The combined organic phase was washed with water (3 mL) and brine (3 mL), dried over Na_2SO_4, filtered, and concentrated in vacuo. The residue was purified by silica column chromatography ($CHCl_3$/MeOH) to give compound **27** (332 mg, 74.1%) as pale yellow solid. ^{1}H NMR (300 MHz, $CDCl_3$) δ 8.60 (s, 1H), 7.39 (s, 1H), 5.82 (ddd, J = 17.1, 10.5, 5.5 Hz, 1H), 5.33 – 5.14 (m, 2H), 4.80 (s, 1H), 4.63 – 4.51 (m, 1H), 4.51 – 4.42 (m, 1H), 4.35 (s, 1H), 1.33 (s, 9H).

***tert*-Butyl (1-(4-amino-5-iodo-7*H*-pyrrolo[2,3-*d*]pyrimidin-7-yl)but-3-en-2-yl) carbamate (28).** To a solution of compound **27** (449 mg, 1.0 mmol) in 1,4-dioxane (10 mL) in a seal tube was added ammonia (10 mL, 25%~28%). The mixture was stirred at 120 ^{o}C for 3 h under pressure. After completion of the reaction, the mixture was cooled to room temperature and was diluted with water (5 mL) and extracted with ethyl acetate (3 × 10 mL). The combined organic phase was washed with brine (5 mL), dried over Na_2SO_4, filtered, and concentrated in vacuo. The residue was purified by silica column chromatography (petroleum ether/EtOAc) to give compound **28** (324 mg, 75.4%) as white solid. ^{1}H NMR (300 MHz, $CDCl_3$) δ 8.25 (s, 1H), 7.05 (s, 1H),

5.87 – 5.74 (m, 1H), 5.72 (s, 2H), 5.34 – 5.13 (m, 3H), 4.56 – 4.43 (m, 1H), 4.34 (dd, J = 14.8, 4.9 Hz, 1H), 4.30 – 4.15 (m, 1H), 1.35 (s, 9H).

***tert*-Butyl (1-(4-amino-5-(4-phenoxyphenyl)-7*H*-pyrrolo[2,3-*d*]pyrimidin-7-yl) but-3-en-2-yl)carbamate (29)**. To a solution of compound **28** (429 mg, 1.0 mmol) in 1,4-dioxane (5 mL) was added (4-phenoxyphenyl)boronic acid (321 mg, 1.5 mmol) and $Pd(PPh_3)_4$ (231 mg, 0.2 mmol). 2N Na_2CO_3 aqueous solution (1 mL, 2.0 mmol) was added. The mixture was stirred at 90 ^oC overnight under N_2. The mixture was cooled to room temperature and diluted with water (5 mL) and extracted with ethyl acetate (3 × 5 mL). The combined organic phase was washed with brine (3 mL), dried over Na_2SO_4, filtered, and concentrated in vacuo. The residue was purified by silica column chromatography ($CHCl_3$/MeOH) to give compound **29** (336 mg, 71.2%) as white solid. ^1H NMR (300 MHz, $CDCl_3$) δ 8.32 (s, 1H), 7.45 – 7.34 (m, 4H), 7.15 (t, *J* = 7.5 Hz, 1H), 7.08 (dd, *J* = 8.4, 1.7 Hz, 4H), 6.95 (s, 1H), 5.84 (ddd, *J* = 16.7, 10.3, 5.4 Hz, 1H), 5.42 (s, 1H), 5.28 (d, *J* = 17.3 Hz, 1H), 5.20 (d, *J* = 10.6 Hz, 1H), 5.13 (s, 2H), 4.64 – 4.50 (m, 1H), 4.36 (s, 2H), 1.32 (s, 9H).

***tert*-Butyl (1-(4-amino-6-bromo-5-(4-phenoxyphenyl)-7*H*-pyrrolo[2,3-*d*] pyrimidin-7-yl)but-3-en-2-yl)carbamate (30).** To a solution of compound **29** (472 mg, 1.0 mmol) in DMF (10 mL) was added *N*-bromosuccinimide (196 mg, 1.1 mmol). The mixture was stirred at room temperature overnight in dark. After completion, the reaction was quenched with water (20 mL) and extracted with ethyl acetate (3 × 5 mL). The combined organic phase was washed with water (5 mL) and brine (5 mL), dried over Na_2SO_4, filtered, and concentrated in vacuo. The residue was purified by

silica column chromatography ($CHCl_3$/MeOH) to give compound **30** (461 mg, 83.8%) as yellowish solid. ^{1}H NMR (300 MHz, $CDCl_3$) δ 8.26 (s, 1H), 7.39 (t, J = 8.2 Hz, 4H), 7.16 (t, J = 7.7 Hz, 1H), 7.09 (d, J = 8.0 Hz, 4H), 5.96 – 5.80 (m, 1H), 5.48 (d, J = 8.4 Hz, 1H), 5.38 – 5.15 (m, 4H), 4.66 (s, 1H), 4.52 – 4.37 (m, 1H), 4.36 – 4.22 (m, 1H), 1.24 (s, 9H).

***tert*-Butyl (4-amino-5-(4-phenoxyphenyl)-6,7,8,9-tetrahydropyrimido[5,4-*b*] indolizin-8-yl)carbamate (31).** To a solution of 9-BBN in dry THF (20 mL, 10.0 mmol) was added compound **30** (550 mg, 1.0 mmol) at 0 ^oC under N_2. The mixture was allowed to warm to room temperature slowly for 5 h. After completion, the mixture was added 3N NaOH aqueous solution (4.7 mL, 14.0 mmol) and Pd(dppf)Cl_2 (190 mg, 0.25 mmol). The mixture was stirred at 85 ^oC for 15 h under N_2, and then quenched with water (10 mL). After extracting with ethyl acetate (3 × 10 mL), the combined organic phase was washed with brine (5 mL), dried over Na_2SO_4, filtered, and concentrated in vacuo. The residue was purified by silica column chromatography (EtOAc) to give compound **31** (232 mg, 49.2%) as yellowish solid. ^{1}H NMR (300 MHz, $CDCl_3$) δ 8.25 (s, 1H), 7.42 – 7.31 (m, 4H), 7.15 (t, J = 7.5 Hz, 1H), 7.08 (d, J = 8.4 Hz, 4H), 5.05 (s, 2H), 4.86 (d, J = 8.0 Hz, 1H), 4.48 (dd, J = 12.6, 4.9 Hz, 1H), 4.27 (s, 1H), 3.94 (dd, J = 12.6, 7.1 Hz, 1H), 3.08 – 2.83 (m, 2H), 2.14 – 2.07 (m, 1H), 1.97 – 1.84 (m, 1H), 1.46 (s, 9H).

***tert*-Butyl (4-amino-6-methylene-5-(4-phenoxyphenyl)-7,8-dihydro-6*H*-pyrimido[5,4-*b*]pyrrolizin-7-yl)carbamate (33).** To a solution of intermediate **30** (550 mg, 1.0 mmol) in THF (15 mL) was added Pd(PPh_3)$_4$ (116 mg, 0.1 mmol). 4N NaOH aqueous solution (3 mL, 12.0 mmol) was then added. The mixture was stirred at 85 ^oC for 15 h under N_2. After quenching with water (10 mL), the mixture was extracted with ethyl acetate (3 × 5 mL). The combined organic phase was washed

with brine (5 mL), dried over Na_2SO_4, filtered, and concentrated in vacuo. The residue was purified by silica column chromatography ($CHCl_3$/MeOH) to give compound **33** (412 mg, 87.8%) as yellowish solid. ^{1}H NMR (300 MHz, $CDCl_3$) δ 8.22 (s, 1H), 7.45 (d, J = 8.6 Hz, 2H), 7.42 – 7.34 (m, 2H), 7.16 (t, J = 7.4 Hz, 1H), 7.09 (d, J = 8.4 Hz, 4H), 5.49 (s, 1H), 5.38 – 5.04 (m, 5H), 4.64 (dd, J = 11.3, 8.0 Hz, 1H), 3.93 (dd, J = 11.4, 5.4 Hz, 1H), 1.47 (s, 9H).

The procedures for synthesis of intermediates **36a-i** are similar to those for synthesis of intermediate **30S** by using **28S** and intermediates **35a-i**. The pinacol esters **35a-i** were prepared by following similar literature procedures.[20f, 25]

Cell Culture. Human lymphoma cell line Ramos was purchased from the American Type Culture Collection (ATCC, Manassas, VA, USA). TMD8 cell was purchased from the Nanjing Cobioer Biological Technology (Nanjing, China). These cells were grown in RPMI-1640 (Gibco®, USA) supplemented with FBS (Gibco®, USA) at 37 °C in humidified 5% CO_2 incubator.

***In Vitro* Enzymatic Activity Assay.** Kinase inhibitory activity of compounds were evaluated using the Enzyme-linked immunosorbent assay (ELISA). The kinase enzyme of BTK, BLK, ErbB4, EGFR, TEC, TXK, ITK, RET, ErbB2, Flt-3, BMX, PDGFR-β, EPH-A2, CSF1R were purchased from Eurofins (Brussels, Belgium) and BTK^{C481S} was bought from SignalChem Lifesciences (British Columbia, Canada). A total of 20 μg/mL Poly (Glu, Tyr) 4:1 (Sigma, St Louis, MO) was precoated in 96-well ELISA plates as a substrate. Active kinases were incubated with indicated drugs in 1×reaction buffer (50 mmol/L HEPES pH 7.4, 20 mmol/L $MgCl_2$, 0.1 mmol/L $MnCl_2$, 0.2 mmol/L Na_3VO_4, 1 mmol/L DTT) containing 5 μmol/L ATP at 37 °C for 1 hour. After incubation, the wells were washed with PBS and then incubated with an anti-phosphotyrosine (PY99) antibody (Santa Cruz Biotechnology,

Santa Cruz, CA) followed by an incubation with horseradish peroxidase (HRP)-conjugated secondary antibody. The wells were visualized using *o*-phenylenediamine (OPD) and the absorbance was read with a multiwell spectrophotometer (VERSAmax™, Molecular Devices, Sunnyvale, CA, USA) at 492 nm.

MTT assay. The cell proliferation Ability was assessed by the thiazolyl blue tetrazolium bromide (MTT) assay. MTT analysis was subsequently performed as per the standard procedures. Briefly, the lymphoma cells were seeded in 96-well plates and grown for 2 h. The cells were then treated with various concentrations of PBS solution containing test compounds, with each concentration tested in triplicate, and then cells were cultured for an additional 72 hours. The IC_{50} values were obtained by using the Logit method and reported as the mean ± SD from three independent determinations.

Kinase Selectivity Profile. The kinase selectivity profile was performed by using the DiscoveRx KINOMEscan platform (http://www.kinomescan.com/).[21] The compound was screened at a concentration of 1 μM against a panel of 468 kinases. The results were defined as a percentage of signal between the negative (DMSO, 100% control) and the positive (control compound, 0% control) control, where the "% control" was calculated as follows: % control = [(test compound signal − positive control signal)/(negative control signal − positive control signal)] × 100.

Western Blot Analysis. Western blot analysis was performed with standard procedures. Briefly, lymphoma cell lines were lysed in SDS lysis buffer and boiled for 30 minutes. Antibodies directed against the following proteins were used: BTK, *p*-BTK (Tyr223), PLCγ2, *p*-PLCγ2 (Tyr759), which were obtained from Cell Signaling Technologies (CST, Cambridge, MA, USA). *β*-Actin and α-tubulin were

obtained from Santa Cruz Biotechnology (Santa Cruz, CA).

Washout Experiment. TMD8 cells were seeded in 6-well plates for 2 hours and exposed to medium containing 1 μM of compound **7S** or ibrutinib. Subsequently, compound **7S** or ibrutinib was removed and cells were washed by PBS for three times. Then the normal medium was added and protein samples were collected at different time points for Western Blot Analysis.

Flow Cytometric Analysis. For the purpose of cell cycle arrest analysis, TMD8 cells were treated with compound **7S** and ibrutinib at the indicated concentrations for 48 h. Cell-cycle arrest was determined by the incorporation of propidium iodide (Sigma-Aldrich) into permeabilized cells. After incubating with drugs for 72 h, cells undergoing apoptosis were identified using an Annexin V-FITC kit (Vazyme Biotech), following the manufacturer's instructions. Both cell cycle arrest and apoptosis were analyzed using a BD Aria III Flow Cytometer (BD Biosciences, San Jose, California, USA). Data were analyzed by Flow Jo software.

***In Vivo* Anti-tumor Activity.** All experiments were performed in compliance with the Animal Ethics Procedures and Guidelines of the People's Republic of China. The mice were maintained under the 12 h light/dark cycles condition in the specific pathogen free (SPF) cleanroom with fresh air (more than 50%), appropriate temperature (20-26 ^{o}C) and humidness (40-70%). All materials and containers were disinfected and sterilized before use. Four- to five-week-old female CB-17 SCID mice were inoculated subcutaneously into the right axilla with TMD8 DLBCL cells (approximately 2×10^6 cells/mouse). When the tumor size reached a volume of ~100-200 mm^3, animals were randomly assigned into control and treated groups (n = 6/group). For efficacy studies, mice in control and in treatment groups were treated with vehicle, compound **1** (25 mg/kg/day) and compound **7S** (5 mg/kg/day; 15

mg/kg/day) for continuous 13, 17, 13 and 17 days, respectively. Tumor burdens were measured by tumor volume. Once tumors reached 20 mm in diameter, mice were sacrificed by CO_2 asphyxiation. Protein level of *p*-BTK (Tyr223) and *p*-PLCγ2 (Tyr759) in tumor were determined using Western blot.

Immunohistochemical (IHC) Assays. Fresh tumor tissues were fixed, embedded in paraffin, and sections (4 μM) were prepared. The immunohistochemical analysis was conducted by Wuhan Goodbio Technology Ltd., and the assay was operated according to the manufacturer's instructions. The quantification of Ki-67 were performed by using the Image Pro.

ASSOCIATED CONTENT

Supporting Information Available. The Supporting information is available free of charge via the Internet at http://pubs.acs.org.

^{1}H and ^{13}C spectra of all new compounds (PDF)

Molecular formula strings (CSV)

AUTHOR INFORMATION

Corresponding Author

For A.Z.: phone: +86-21-50806035; fax: 86-21-50806035; E-mail: aozhang@simm.ac.cn.

For H.X.: phone: +86-21-50805897; fax: 86-21-50805897; E-mail: hxie@simm.ac.cn.

For L.S.: phone: +86-25-83271414; fax: 86-25-83271414; Email: chslp@cpu.edu.cn

Author Contributions

Y.X., P.S., and Z.S. contributed equally to this work.

Notes

The authors declare no competing financial interest.

ACKNOWLEDGEMENT

This work was supported by grants from Chinese NSF (Grants 81430080, 81773565, 81703327). Supporting grants from the International Cooperative Program (Grant GJHZ1622) and Key Program of the Frontier Science (Grant 160621) of the Chinese Academy of Sciences, the Shanghai Commission of Science and Technology (Grants 16XD1404600, 14431900400), Jiangsu University Excellent Scientific and Technological Innovation Team (2015) as well as Postgraduate Research & Practice Innovation Program of Jiangsu Province (KYCX17_0684) are also appreciated.

ABBREVIATIONS USED

BTK, Bruton's tyrosine kinase; BCR, B-cell receptor; RTV, Relative Tumor Volume; MCL, mantle cell lymphoma; CLL, chronic lymphocytic leukemia; EGFR, epidermal growth factor receptor; PK, pharmacokinetic; V_{ss}, volume of distribution; $T_{1/2}$, half-life; C_{max}, maximum concentration; T_{max}, time of maximum concentration; $AUC_{0-\infty}$, area under the plasma concentration time curve; *F*, oral bioavailability; MLM, mouse liver microsome; HLM, human liver microsome; RLM, rat liver microsome; SYK, spleen tyrosine kinase; PLCγ2, phospholipase γ2; DLBCL, diffuse large B-cell lymphoma; QD, once daily; MesCl, methanesulfonyl chloride; NBS, N-bromobutanimide; TFA, trifluoroacetic acid; 9-BBN, 9-borabicyclo[3.3.1]nonane; HATU, 1-[bis(dimethylamino)methylene]-1*H*-1,2,3-triazolo[4,5-*b*]pyridinium-3-oxid hexafluorophosphate; DACH-naphthyl, 1,2-diaminocyclohexane-*N*,*N*'-bis(2-diphenyl phosphino-1-naphthoyl); PBS, phosphate buffer saline; SPF, specific pathogen free; IHC, immunohistochemical.

REFERENCES

1. Smith, C. I. E.; Islam, T. C.; Mattsson, P. T.; Mohamed, A. J.; Nore, B. F.; Vihinen M. The Tec family of cytoplasmic tyrosine kinases: mammalian Btk, Bmx, Itk, Tec, Txk and homologs in other species. *Bioessays* **2001**, *23*, 436-446.

2. (a) Satterthwaite, A. B.; Witte, O. N. The role of Bruton's tyrosine kinase in B-cell development and function: A genetic perspective. *Immunol. Rev.* **2000**, *175*, 120-127. (b) Khan, W. N. Regulation of B lymphocyte development and activation by Bruton's tyrosine kinase. *Immunol. Res.* **2001**, *23*, 147-156.
3. Smith, C. I. E.; Baskin, B.; Humire-Greiff, P.; Zhou, J. N.; Olsson, P. G.; Maniar, H. S.; Kjellén, P.; Lambris, J. D.; Christensson, B.; Hammarström, L.; Bentley, D.; Vetire, D.; Islam, K. B.; Vorechovský, I.; Sideras, P. Expression of Bruton's agammaglobulinemia tyrosine kinase gene, BTK, is selectively down-regulated in T lymphocytes and plasma cells. *J. Immunol.* **1994**, *152*, 557-565.
4. (a) Küppers, R. Mechanisms of B-cell lymphoma pathogenesis. *Nat. Rev. Cancer* **2005**, *5*, 251-262. (b) Davis, R. E.; Ngo, V. N.; Lenz1, G.; Tolar, P.; Young, R. M.; Romesser, P. B.; Kohlhammer, H.; Lamy, L.; Zhao, H.; Yang, Y. D.; Xu, W. H.; Shaffer, A. L.; Wright, G.; Xiao, W. M.; Powell, J.; Jiang, J. K.; Thomas, C. J.; Rosenwald, A.; Ott, G.; Muller-Hermelink, H. K.; Gascoyne, R. D.; Connors, J. M.; Johnson, N. A.; Rimsza, L. M.; Campo, E.; Jaffe, E. S.; Wilson, W. H.; Delabie, J.; Smeland, E. B.; Fisher, R. I.; Braziel, R. M.; Tubbs, R. R.; Cook, J. R.; Weisenburger, D. D.; Chan, W. C.; Pierce, S. K.; Staudt, L. M. Chronic active B-cell-receptor signalling in diffuse large B-cell lymphoma. *Nature* **2010**, *463*, 88-92. (c) Niemann, C. U.; Wiestner, A. B-cell receptor signaling as a driver of lymphoma development and evolution. *Semin. Cancer Biol.* **2013**, *23*, 410-421.
5. (a) Pan, Z. Y.; Scheerens, H.; Li, S. J.; Schultz, B. E.; Sprengeler, P. A.; Burrill, L. C.; Mendonca, R. V.; Sweeney, M. D.; Scott, K. C. K.; Grothaus, P. G.; Jeffery, D.

A.; Spoerke, J. M.; Honigberg, L. A.; Young, P. R.; Dalrymple, S. A.; Palmer, J. T. Discovery of selective irreversible inhibitors for Bruton's tyrosine kinase. *ChemMedChem* **2007**, *2*, 58-61. (b) Honigberg, L. A.; Smith, A. M.; Sirisawad, M.; Verner, E.; Lourya, D.; Chang, B.; Li, S.; Pan, Z. Y.; Thamm, D. H.; Miller, R. A.; Buggy, J. J. The Bruton tyrosine kinase inhibitor PCI-32765 blocks B-cell activation and is efficacious in models of autoimmune disease and B-cell malignancy. *Proc. Natl. Acad. Sci. USA.* **2010**, *107*, 13075-13080.

6. (a) Brown, J. R. Ibrutinib (PCI-32765), the first BTK (Bruton's tyrosine kinase) inhibitor in clinical trials. *Curr. Hematol. Malig. Rep.* **2013**, *8*, 1-6. (b) Drug@FDA, New Drug Application 2055520 Pharmacology Review(s).
7. Aw, A.; Brown, J. R. Current status of Bruton's tyrosine kinase inhibitor development and use in B-cell malignancies. *Drugs Aging* **2017**, *34*, 509-527.
8. Wu, J. J.; Liu, C.; Tsui, S. T.; Liu, D. L. Second-generation inhibitors of Bruton tyrosine kinase. *J. Hematol. Oncol.* **2016**, *9*, 80-86.
9. (a) Wu, J. J.; Zhang, M. Z.; Liu, D. L. Acalabrutinib (ACP-196): a selective second-generation BTK inhibitor. *J. Hematol. Oncol.* **2016**, *9*, 21-25. (b) Herman, S. E. M.; Montraveta, A.; Niemann, C. U.; Mora-Jensen, H.; Gulrajani, M.; Krantz, F.; Mantel, R.; Smith, L. L.; McClanahan, F.; Harrington, B. K.; Colomer, D.; Covey, T.; Byrd, J. C.; Izumi, R.; Kaptein, A.; Ulrich, R.; Johnson, A. J.; Lannutti, B. J.; Wiestner, A.; Woyach, J. A. The Bruton tyrosine kinase (BTK) inhibitor acalabrutinib demonstrates potent on-target effects and efficacy in two mouse models of chronic lymphocytic leukemia. *Clin. Cancer Res.* **2017**, *23*, 2831-2841.

10. (a) Yasuhiro, T.; Yoshizawa, T.; Hotta, S.; Ariza, Y.; Ueda, Y.; Kozaki, R.; Birkett, J. Abstract 2452: ONO-4059, a novel oral Bruton's tyrosine kinase (Btk) inhibitor that demonstrates potent pharmacodynamic activity through Phosphorylated Btk (P-Btk) inhibition, in addition to effective anti-tumour activity in a TMD-8 (DLBCL) xenograft model. *Cancer Res.* **2013**, *73*(8 Supplement): 2452. (b) Walter, H. S.; Rule, S. A.; Dyer, M. J. S.; Karlin, L.; Jones, C.; Cazin, B.; Quittet, P.; Shah, N.; Hutchinson, C. V.; Honda, H.; Duffy, K.; Birkett, J.; Jamieson, V.; Courtenay-Luck, N.; Yoshizawa, T.; Sharpe, J.; Ohno, T.; Abe, S.; Nishimura, A.; Cartron, G.; Morschhauser, F.; Fegan, C.; Salles, G. A phase 1 clinical trial of the selective BTK inhibitor ONO/GS-4059 in relapsed and refractory mature B-cell malignancies. *Blood* **2016**, *127*, 411-419.

11. Evans, E. K.; Tester, R.; Aslanian, S.; Karp, R.; Sheets, M.; Labenski, M. T.; Witowski, S. R.; Lounsbury, H.; Chaturvedi, P.; Mazdiyasni, H.; Zhu, Z. D.; Nacht, M.; Freed, M. I.; Petter, R. C.; Dubrovskiy, A.; Singh, J.; Westlin, W. F. Inhibition of BTK with CC-292 provides early pharmacodynamic assessment of activity in mice and humans. *J. Pharmacol. Exp. Ther.* **2013**, *346*, 219-228.

12. Byrd, J. C.; Harrington, B.; O'Brien, S.; Jones, J. A.; Schuh, A.; Devereux, S.; Chaves, J.; Wierda, W. G.; Awan, F. T.; Brown, J. R.; Hillmen, P.; Stephens, D. M.; Ghia, P.; Barrientos, J. C.; Pagel, J. M.; Woyach, J.; Johnson, D.; Huang, J.; Wang, X. L.; Lannutti, B. J.; Covey, T.; Fardis, M.; McGreivy, J.; Hamdy, A.; Rothbaum, W.; Izumi, R.; Diacovo, T. G.; Johnson, A. J.; Furman, R. R. Acalabrutinib (ACP-196) in relapsed chronic lymphocytic leukemia. *N. Engl. J. Med.* **2016**, *374*,

323-332.

13. Lou, Y.; Han, X. C.; Kuglstatter, A.; Kondru, R. K.; Sweeney, Z. K.; Soth, M.; McIntosh, J.; Litman, R.; Suh, J.; Kocer, B.; Davis, D.; Park, J.; Frauchiger, S.; Dewdney, N.; Zecic, H.; Taygerly, J. P.; Sarma, K.; Hong, J.; Hill, R. J.; Gabriel, T.; Goldstein, D. M.; Owens, T. D. Structure-based drug design of RN486, a potent and selective Bruton's tyrosine kinase (BTK) Inhibitor, for the treatment of rheumatoid arthritis. *J. Med. Chem.* **2015**, *58*, 512-516.

14. Di Paolo, J. A.; Huang, T.; Balazs, M.; Barbosa, J.; Barck, K. H.; Bravo, B. J.; Carano, R. A. D.; Darrow, J.; Davies, D. R.; DeForge, L. E.; Diehl, L.; Ferrando, R.; Gallion, S. L.; Giannetti, A. M.; Gribling, P.; Hurez, V.; Hymowitz, S. G.; Jones, R.; Kropf, J. E.; Lee, W. P.; Maciejewski, P. M.; Mitchell, S. A.; Rong, H.; Staker, B. L.; Whitney, J. A.; Yeh, S.; Young, W. B.; Yu, C.; Zhang, J.; Reif, K.; Currie, K. S. Specific Btk inhibition suppresses B cell- and myeloid cell-mediated arthritis. *Nat. Chem. Biol.* **2011**, *7*, 41-50.

15. Crawford, J. J.; Johnson, A. R.; Misner, D. L.; Belmont, L. D.; Castanedo, G.; Choy, R.; Coraggio, M.; Dong, L. M.; Eigenbrot, C.; Erickson, R.; Ghilardi, N.; Hau, J.; Katewa, A.; Kohli, P. B.; Lee, W.; Lubach, J. W.; McKenzie, B. S.; Ortwine, D. F.; Schutt, L.; Tay, S.; Wei, B. Q.; Reif, K.; Liu, L. C.; Wong, H.; Young, W. B. Discovery of GDC-0853: a potent, selective, and noncovalent Bruton's tyrosine kinase inhibitor in early clinical development. *J. Med. Chem.* **2018**, *61*, 2227-2245.

16. Lou, Y.; Owens, T. D.; Kuglstatter, A.; Kondru, R. K.; Goldstein, D. M. Bruton's

tyrosine kinase inhibitors: approaches to potent and selective inhibition, preclinical and clinical evaluation for inflammatory diseases and B cell malignancies. *J. Med. Chem.* **2012**, *55*, 4539-4550.

17. (a) Smith, C. R.; Dougan, D. R.; Komandla, M.; Kanouni, T.; Knight, B.; Lawson, J. D.; Sabat, M.; Taylor, E. R.; Vu, P.; Wyrick, C. Fragment-based discovery of a small molecule inhibitor of Bruton's tyrosine kinase. *J. Med. Chem.* **2015**, *58*, 5437-5444. (b) Li, X. T.; Zuo, Y. Y.; Tang, G. H.; Wang, Y.; Zhou, Y. Q.; Wang, X. Y.; Guo, T. L.; Xia, M. Y.; Ding, N.; Pan, Z. Y. Discovery of a series of 2,5-diaminopyrimidine covalent irreversible inhibitors of Bruton's tyrosine kinase with in vivo antitumor activity. *J. Med. Chem.* **2014**, *57*, 5112-5128. (c) Watterson, S. H.; De Lucca, G. V.; Shi, Q.; Langevine, C. M. Liu, Q. J.; Batt, D. G.; Bertrand, M. B.; Gong, H.; Dai, J.; Yip, S. H.; Li, P.; Sun, D.; Wu, D. R.; Wang, C. L.; Zhang, Y. R.; Traeger, S. C.; Pattoli, M. A.; Skala, S.; Cheng, L. H.; Obermeier, M. T.; Vickery, R.; Discenza, L. N.; D'Arienzo, C. J.; Zhang, Y. F.; Heimrich, E.; Gillooly, K. M.; Taylor, T. L.; Pulicicchio, C.; McIntyre, K. W.; Galella, M. A.; Tebben, A. J.; Muckelbauer, J. K.; Chang, C. Y.; Rampulla, R.; Mathur, A.; Salter-Cid, L.; Barrish, J. C.; Carter, P. H.; Fura, A.; Burke, J. R.; Tino, J. A. Discovery of 6-fluoro-5-(*R*)-(3-(*S*)-(8-fluoro-1-methyl-2,4-dioxo-1,2-dihydro quinazolin-3(4*H*)-yl)-2-methylphenyl)-2-(*S*)-(2-hydroxypropan-2-yl)-2,3,4,9-tetra hydro-1*H*-carbazole-8-carboxamide (BMS-986142): a reversible inhibitor of Bruton's tyrosine kinase (BTK) conformationally constrained by two locked atropisomers. *J. Med. Chem.* **2016**, *59*, 9173-9200. (d) Wan, H. L.; Wang, Z. R.; Li,

L. L.; Cheng, C.; Ji, P.; Liu, J. J.; Zhang, H.; Zou, J.; Yang, S. Y. Discovery of novel Bruton's tyrosine kinase inhibitors using a hybrid protocol of virtual screening approaches based on SVM model, pharmacophore and molecular docking. *Chem. Biol. Drug Des.* **2012**, *80*, 366-373.

18. (a) Uno, T.; Nonoshita, K.; Shimamura, T. Novel Quinolone-substituted Compound. WO 2015/025936 A1, Feb 26, 2015. (b) Wang, C. Y.; Liu, H. C.; Song, Z. L.; Ji, Y. C.; Xing, L.; Peng, X.; Wang, X. S.; Ai, J.; Geng, M. Y.; Zhang, A. Synthesis and structure-activity relationship study of pyrazolo[3,4-*d*]pyrimidines as tyrosine kinase RET inhibitors. *Bioorg. Med. Chem. Lett.* **2017**, *27*, 2544-2548.

19. Marcotte, D. J.; Liu, Y. T.; Arduini, R. M.; Hession, C. A.; Miatkowski, K.; Wildes, C. P.; Cullen, P. F.; Hong, V.; Hopkins, B. T.; Mertsching, E.; Jenkins, T. J.; Romanowski, M. J.; Baker, D. P.; Silvian, L. F. Structures of human Bruton's tyrosine kinase in active and inactive conformations suggest a mechanism of activation for TEC family kinases. *Protein Sci.* **2010**, *19*, 429-439.

20. (a) Konteatis, Z.; Moffett, K.; Lee, Y. H.; Chao, W. C. Pyrrolotriazine Compounds. WO 2010/126960 A1, Nov 4, 2010. (b) Bui, M.; Conlon, P.; Erlanson, D. A.; Fan, J. F.; Guan, B.; Hopkins, B. T.; Ishchenko, A.; Jenkins, T. J.; Kumaravel, G.; Marcotte, D.; Powell, N.; Scott, D.; Taveras, A.; Wang, D. P.; Zhong, M. Heteroaryl Btk Inhibitors. WO 2011/029043 A1, Mar 10, 2011. (c) Gaillard, P.; Seenisamy, J.; Liu-Bujalski, L.; Potnick, J.; Caldwell, R. D.; Qiu, H.; Neagu, C.; Jones, R.; Won, A. C.; Goutopoulos, A.; Sherer, B. A.; Johnson, T. L.; Gardberg, A. Heteroaryl Compounds as Btk Inhibitors and Uses Thereof. WO 2016/057500 A1,

Apr 14, 2016. (d) Liao, X. B.; Li, J.; Lu, Z. J.; Zhou, Y. B.; Gao, A. H. Bruton's Tyrosine Kinase Inhibitors. WO 2017/127371 A1, Jul 27, 2017. (e) Zhao, X. G.; Xin, M. H.; Wang, Y. Z.; Huang, W.; Jin, Q.; Tang, F.; Wu, G.; Zhao, Y.; Xiang, H. Discovery of thieno[3,2-*c*]pyridin-4-amines as novel Bruton's tyrosine kinase (BTK) inhibitors. *Bioorg. Med. Chem.* **2015**, *23*, 6059-6068. (f) Liu, J.; Guiadeen, D.; Krikorian, A.; Gao, X. L.; Wang, J.; Boga, S. B.; Alhassan, A. B.; Yu, Y. N.; Vaccaro, H.; Liu, S. L.; Yang, C. D.; Wu, H.; Cooper, A.; de Man, J.; Kaptein, A.; Maloney, K.; Hornak, V.; Gao, Y. D.; Fischmann, T. O.; Raaijmakers, H.; Vu-Pham, D.; Presland, J.; Mansueto, M.; Xu, Z. W.; Leccese, E.; Zhang-Hoover, J.; Knemeyer, I.; Garlisi, C. G.; Bays, N.; Stivers, P.; Brandish, P. E.; Hicks, A.; Kim, R.; Kozlowski, J. A. Discovery of 8‑amino-imidazo[1,5-*a*]pyrazines as reversible BTK inhibitors for the treatment of rheumatoid arthritis. *ACS Med. Chem. Lett.* **2016**, *7*, 198-203.

21. Fabian, M. A.; Biggs III, W. H.; Treiber, D. K.; Atteridge, C. E.; Azimioara, M. D.; Benedetti, M. G.; Carter, T. A.; Ciceri, P.; Edeen, P. T.; Floyd, M.; Ford, J. M.; Galvin, M.; Gerlach, J. L.; Grotzfeld, R. M.; Herrgard, S.; Insko, D. E.; Insko, M. A.; Lai, A. G.; Lélias, J. M.; Mehta, S. A.; Milanov, Z. V.; Velasco, A. M.; Wodicka, L. M.; Patel, H. K.; Zarrinkar, P. P.; Lockhart, D. J. A small molecule-kinase interaction map for clinical kinase inhibitors. *Nat. Biotechnol.* **2005**, *23*, 329-336.

22. Wang, Y.; Zhang, L. L.; Champlin, R. E.; Wang, M. L. Targeting Bruton's tyrosine kinase with ibrutinib in B-cell malignancies. *Clin. Pharmacol. Ther.* **2015**, *97*,

455-468.

23. Scholzen, T.; Gerdes, J. The Ki-67 protein: from the known and the unknown. *J. Cell Physiol.* **2000**, *182*, 311-322.

24. Trost, B. M.; O'Boyle, B. M.; Torres, W.; Ameriks, M. K. Development of a flexible strategy towards FR900482 and the mitomycins. *Chem. Eur. J.* **2011**, *17*, 7890-7903.

25. Chen, X. Y.; Gao, Y. X.; Liu, C.; Ni, H. H.; Mulvihill, M. Substituted Nicotinimide Inhibitors of Btk and Their Preparation and Use in the Treatment of Cancer, Inflammation and Autoimmune Disease. WO 2015/048662 A2, Apr 2, 2015.

Table of Content Graphic